GENERAL
ENGINEERING
LABORATORY

ON THE LOAD CAPACITY AND STABILITY OF ROTORS IN CYLINDRICAL GAS-DYNAMIC JOURNAL BEARINGS

BY

B. STERNLICHT
L. W. WINN

JULY 3, 1961

GENERAL ELECTRIC

GL-316A (4-59)

General Engineering Laboratory

ON THE LOAD CAPACITY AND STABILITY OF ROTORS IN CYLINDRICAL GAS-DYNAMIC JOURNAL BEARINGS

by

B. Sternlicht
L. W. Winn

July 3, 1961

Technical Report

For: Office of Naval Research
Contract No.: NONR 2844(00)
Task No.: NR 097-348

GENERAL ELECTRIC
SCHENECTADY, NEW YORK

TABLE OF CONTENTS

NOMENCLATURE

b	M/W
C	Radial Clearance, 1 inch
F	Bearing Load, lbs.
HFW	Half Frequency Whirl
I_P	Polar Moment of Inertia, #-sec.^{2} - in.
I_T	Translatory Moment of Inertia, #-sec.^{2} - in.
K_2	Radial Bearing Stiffness, #/inch
K_c	Radial Translatory Stiffness Evaluated at ω_c, #/inch
ℓ	Bearing Span, inches
L	Bearing Length, inches
m	Mass, $\frac{\#\text{-sec.}^2}{\text{inch}}$
P_a	Ambient Pressure, psia
R	Bearing Radius, inches
ϵ	Eccentricity Ratio
Λ	Compressibility Number
μ	Viscosity, $\frac{\#\text{-sec.}}{\text{in.}^2}$
$\emptyset$	Attitude Angle, degrees
ω	Angular Velocity, rad/sec
ω_c	Angular Velocity at Onset of HFW - conical whip, rad/sec
ω_T	Angular Velocity at Onset of HFW - translatory whip, rad/sec

INTRODUCTION

In order that gas bearings become more widely applied, it is necessary to gain a better understanding of their dynamic characteristic. One of the most troublesome phenomena that is often exhibited with rotors operating in gas bearings is that of Half Frequency Whirl instability. We have taken a two pronged attack on this problem employing theory and experiment. This report presents our experimental results and compares them to other available experimental data and theory. In this way we hope to compliment these two approaches and clarify this difficult problem.

Eccentricity and attitude angle tests for steady load are also reported here. These were conducted to assure ourselves that good correlation between theory and experiment exists and that our measurements are accurate. Initial disturbance and "actual onset" of Half Frequency Whirl were measured for a variety of conditions. The effect of load, mass, L/D, and clearance on the threshold of instability was established and compared with theory.

I. OBJECTIVES

These tests were designed to meet the following objectives:

1. Verify through test, analysis of eccentricity and attitude angle of self acting bearings as outlined in Ref. 1, and 2, varying bearing clearance, L/D, load and speed.
2. Compare results, obtained through analytical methods (Ref. 3), for onset of half frequency whirl with results obtained on test varying load, mass and bearing geometry.

II. TEST EQUIPMENT

The test rig used in this series of tests consists of a housing and rotor as shown in Fig. 1. An air impulse turbine similar to a Terry turbine is used to drive the rotor. The turbine wheel mounts on the shaft fastened through a pair of Woodruff keys and locked in place by locknuts, as shown in Fig. 2. In order to minimize aerodynamic forces full arc admission is employed. The nozzle box is mounted on housing guided by a rabbet arrangement. For the purpose of rotor balance and reversal of rotation an identical dummy turbine wheel is mounted on the other end of the rotor. The rotor is restrained from axial motion through the use of two thrust plates. Both of these plates are externally pressurized. The thrust plate drawing is shown in Fig. 3.

The entire housing is mounted in a wooden block which in turn is fastened to two parallel steel plates in such a manner that bearing load variation can be accomplished through mounting of the housing in an inclined position. The housing can be inclined from 0^{o} (horizontal) to 90^{o} (vertical) in 15^{o} increments, yielding a load variation running from full rotor weight as the bearing load for the horizontal position to zero bearing load in the vertical position. Fig. 4 shows a side view of the assembled test rig and instrumentation.

The test fixture has been provided with two rotors for purposes of variation of mass and inertia. One rotor, including turbine wheel, is made of 4340 steel as is the entire rig, the other of 7075-T6 aluminum.

Two bearings, the length and clearance of which can be readily changed, are shrink fitted into the housing. Each bearing was provided with a single 0.020" diameter orifice and 3/32" long. The purpose of the orifice was to prevent rubbing at start ups and coast downs. It could also be employed for

control of whirl amplitude so as to prevent rotor-bearing contact. The bearing orifice configuration in bearings with L/D ratio of 2 is shown in Fig. 5. Due to effects of orifice on onset of half frequency whirl bearings with L/D ratio of 1 have been redesigned to facilitate plugging of the orifice. This arrangement is also shown in Fig. 5.

Particular attention was paid to the roundness, finish and alignment of the journal bearings. The bearings were made of leaded bronze and finished by lapping to called-for tolerances. Checks on roundness and alignment were performed on an Indiron. This instrument permits resolutions of bearing inaccuracies up to 10 Micro-inches. All roundness and alignment between bearings were kept to within 50 Micro-inches maximum. The results of the Indiron measurements were checked against air gage measurements.

Rotor balance was performed on air bearing mounts in a Gishold balancing machine. Maximum rotor unbalance amounted to 0.1 gm-inches.

Inertia effects on onset of half frequency whirl had to be taken into consideration in the test rig design. It was presumed that if onset of half frequency whirl results in conical modes of rotor oscillation, the double thrust plate arrangement may have a restraining effect on the onset of whirl rendering comparison with analytical results difficult. In line with this reasoning, an attempt was made to insure that translatory whirl will set in at lower speeds than conical. Equations derived in Ref. 4 were used to obtain translatory whirl.

According to Ref. 4:

$$\frac{\omega_T}{\omega_c} = \frac{12(I_T - 2I_P)K_2}{m(3\ell^2 + L^2)K_c} \qquad (1)$$

This indicates that when the right hand side of the equation is smaller than 1, translatory whirl will take place. Since the dynamic radial bearing stiffnesses, K_2 and K_c for the translatory and conical modes of vibration could not be evaluated at the time the tests were initiated due to unavailability of data, the value of equation (1) with exception of the K_2/K_c ratio had to be kept as low as possible. The inertias, masses, and value of equation (1) with factor K_2/K_c out are given below:

	Al, Rotor	Steel Rotor
I_P #-sec.^{2} - in.	0.0095	0.0267
I_T #-sec.^{2} - in.	0.9444	2.6461
m $\frac{\#\text{-sec.}^2}{\text{in.}}$	0.0192	0.0537
$\frac{12(I_T - 2I_P)}{m(3\ell^2 + L^2)}$	0.749	0.739

In our testing, the onset of half frequency whirl was translatory with a few exceptions shown in the discussion of test results.

In summary the test equipment was designed sufficiently versatile so that the following parameters could be investigated:

1.) Bearing geometry
   a.) L/D
   b.) clearance
   c.) grooving, non-circulatory, etc.
2.) Bearing span
3.) Attitude of load with respect to geometric irregularity within the bearing
4.) Load

5.) Mass

6.) Inertia

7.) Speed - 0-100,000 rpm

III. INSTRUMENTATION

Four capacitive probes on each end of the housing were used for the purpose of determination of shaft center location within the clearance circle, which in turn permits one to determine eccentricity ratio and attitude angle.

The probes were paired prior to mounting, and adjusted to yield linear output over specified displacement. When mounted in housing each set of horizontal and vertical pairs was connected to a Fielden Proximity Meter. Fielden outputs of the horizontal and vertical pairs of probes on each bearing were then connected to the X and Y inputs of scopes and calibrated over the displacement range with the help of precision measuring Indiac's mounted on each side of the housing. As a final check on calibration, the housing was rotated with respect to rotor causing the signal on the CRO screen to follow a perfect circle corresponding to the clearance circle. This method of checkout has proven extremely useful since either irregularities, non-linearity or foreign material within the clearance space could be easily detected. In all tests save No. 4, each division on the scope screen corresponded to 100 Micro-inches. In Test No. 4 due to large bearing clearance the value of Micro-inches per graduation was increased to 200. The errors involved in the measuring system (drifts and readings) are estimated to be below 50 Micro-inches. This gives higher percentage of error for low eccentricity ratios.

After each run, calibration was rechecked and, if departures from original calibration were found, the tests were repeated until it was made certain that original calibration was maintained throughout and after the run. This procedure helped to eliminate drift and calibration error.

In order to determine the mode of half frequency whirl the Fielden outputs of both sets of vertical probes (both bearings) were fed into A and B channels

of a dual beam scope and simultaneously displayed on the same time base permitting determination of phase angle between rotor ends. This information combined with amplitude readings off the CRO screens determined the position of the rotor axis.

The frequency of shaft oscillation during half frequency whirl was measured through the comparison of a known frequency signal fed into a scope with output of one set of capacitive probes. The known frequency signal was supplied by an oscillator, the output of which was rechecked on an Eput meter.

Preliminary tests were performed to determine the influence of thrust plates and nozzle box air inlet on the onset of half frequency whirl. Thrust plate supply pressure was varied from 10-90 psi with no measurable effect on the onset of HFW. The air inlet into the nozzle box was rotated through 360^{o} and no effects of same on onset of HFW could be found.

Special precautions were taken to assure that test rig will operate in a vibration free environment. The rig was mounted on a heavy steel table which in turn was placed on vibration isolation pads to reduce the effect of building vibration. Despite these precautions some slight vibrations were transmitted at times. In some tests it was noted that initial disturbance indicating onset of half frequency whirl occurred at speeds lower than the actual inception of half frequency whirl as determined by the continuous growth of the whirl amplitude. When this borderline region of instability existed the presence of vibration could excite the half frequency whirl at speeds as much as 500 rpm lower than if the external vibrations were absent.

IV. DISCUSSION OF TEST RESULTS

A. Load Carrying Capacity - Steady Radial Load

The tests were started with plain cylindrical journal bearings of L/D ratio of 2 (D = 2", L = 4") and average radial clearance of 0.000611". After all data on this configuration was obtained, the clearance was opened to 0.001". For subsequent tests the bearings were replaced with sleeves of L/D of 1 and clearance of 0.000611" after which again the clearance was opened to 0.001147". The test sequence as described is thus consecutively numbered as Tests 1, 2, 3 and 4; A, B, and C, the test number applying to a specific bearing geometry and letters to different loads. Each test was performed with an aluminum and steel rotor of similar dimensions (to within 40 microinches).

For purposes of elimination of rubbing contact at start up and coast down high pressure air was applied to an orifice and after the rotor was brought up to speed fittings were sealed off so that orifice remained sealed save for its connection to the annular groove in tests 1 and 2. In tests 3 and 4, the sealing arrangement was revised so that the annular groove was eliminated and orifice was sealed directly on the bearing outside diameter. The lifting and orifice and the static load in phase will be henceforth referred to as the 0° position, thus the 180° position will have the orifice located on top of the bearing 180° away from the normal load direction. In order to eliminate external friction and damping normally encountered with external load application, the bearing load was that due to the rotor weight only, and variations in load were obtained through variation of housing position.

The load carrying capacity data obtained in tests 1 through 4 is given in tables 1 - 12. Dimensionless parameters were calculated and the results of Λ vs. ϵ and $\emptyset$ are plotted in Figs. 6-9. Theoretical values of $\emptyset$ obtained from reference 1 are also plotted in these figures for comparison. In general the agreement between theoretical and test attitude angles runs from fair to excellent the maximum discrepancy not exceeding 18^{o}. No definite trend in the departure of test values from calculated values could be established which seems to suggest that the discrepancies are due to random occurrence of combination of errors such as those due to out of roundness of bearings and rotor, misalignment and measuring system.

The random distribution of errors can be more readily seen from the plot of Λ vs. f at different eccentricity ratios, obtained from Ref. 2 and shown in Figs. 14 and 15 on which tests points were superimposed. These points were crossplotted from Figs. 6-13 for eccentricity ratios of .2, .3, .4, etc. The plots indicate good agreement at low eccentricity ratios, however, as the eccentricity ratio increases, the scatter of data points becomes more pronounced. It can be seen that at high eccentricity ratios on bearings with larger clearance a maximum difference of 16% in load carrying capacity between test and theory exists.

This may well be due to the fact that at low minimum film thicknesses (high eccentricity ratio) effects of bearing and rotor manufacturing inaccuracies become proportionately more significant thus contributing to the scatter of data in a random fashion.

Summarizing: It is felt that static load carrying capacity tests for plain cylindrical journal bearings agree well with isothermal theory. Slight departures of test values from theory might be explained in terms of errors due to imperfection of bearings and measuring system.

V. HALF FREQUENCY WHIRL RESULTS - STEADY RADIAL LOAD

The half frequency whirl tests are numbered 5 through 12, A through E, the number denoting the L/D ratio and clearance and letters denoting applied bearing load. Half frequency whirl tests were performed on the same set up as the load carrying capacity tests. Onsets (or threshold) of half frequency whirl were obtained for the same bearing geometries as in the load carrying capacity tests and for various bearing loads. A number of problems were encountered which for the purpose of clarification are described below.

A. Clearance Effect

In order to scan the effects of bearing clearance on the onset of half frequency whirl tests with radial clearances of 0.000445", 0.000771" and 0.00122" for L/D ratio of 2 and 0.001643" for L/D ratio of 1 had to be performed in addition to the tests described in the section on load carrying capacity. The results definitely indicate the existence of a clearance which gives minimum onset frequency for a given bearing load. On either side of this clearance the threshold of half frequency whirl is greater. It should be pointed out that an analyses of stability performed in parallel with this test program confirmed this observation (Ref. 3).

B. Orifice Effects

One of the problems encountered in determination of the onset of half frequency whirl was that of the effect of the 0.020" diameter orifice located in the center of each bearing as previously described. The orifice was incorporated into the test design to perform the following functions:

a. With pressurized orifice, rubbing at start off and coast down was eliminated.

b. Excessive growth of amplitude at half frequency whirl could be controlled through the application of external pressure, thus preventing damage to shaft and bearings.

Our past experience with half frequency whirl tests indicated that whenever those precautions were not taken damage to shaft and bearings would occur and data subsequently obtained could not be relied upon. The orifice, however, introduces other problems, which definitely do affect the quantitative test results. Orifice effects are described in more detail in the discussion of test data and Ref. 5.

C. Determination of Point of Onset of HFW

In tests with the orifice in the 0^{o} position (in line with load), half frequency whirl set in and kept on growing in amplitude as speed increased. The point at which growth in amplitude became apparent and continued with increase in speed was denoted as the "actual onset". This in most of the cases in 0^{o} position corresponded to the initial disturbance observed on the scope screen.

In some cases, however, as in tests No. 7, 9 for L/D = 2, and aluminum rotor tests for L/D = 1, an initial disturbance indicating instability occurred at speeds lower than the "actual onset" of half frequency whirl as determined by the continuous growth of whirl amplitude. It was also noted that once the initial disturbance registered on the screen, the rotor exhibited a tendency to go in and out of whirl, and external disturbances in the form of vibrations or sudden sharp blows could produce self sustained half frequency whirl.

These observations lead one to conclude that the actual onset of instability in the absence of external damping or body forces does occur at the speed at which initial disturbance is exhibited. The half frequency results presented in this report for the 0^{o} position are based upon the speed at which initial disturbance took place. Whenever some did not coincide with the "actual onset" two values of speed are given, one representing the initial disturbance and the other the "actual onset". In the 180^{o} orifice position the initial disturbances still occurred at the same speeds as in the 0^{o} position, but these were quickly damped out to the point where stable operation was possible up to speeds considerably above the 0^{o} position limits. The values given for onset of HFW in 180^{o} position are thus based upon "actual onset" accompanied by growth in amplitude of whirl with speed. All onset speeds are subject to an error of $\pm$200 RPM mainly due to factors involved in interpretation of onset speed.

Plugging of the 0.020" diameter orifice resulted in increased onset speed in 0^{o} position and decrease of onset speeds in the 180^{o} position, in no case, however, were the two onsets identical, nor was the initial disturbance at the low speeds with the orifice open and in 0^{o} position, eliminated. This indicates that bearing imperfections of the size of the orifice influence the threshold of instability and that relatively small external body forces can suppress the onset of half frequency whirl.

D. Operation in Region of HFW

Once half frequency whirl was established operation within the region of instability appeared to be a function of many variables. Although exploration of bearing performance within the region of half frequency whirl was not an objective of this phase of the program a few observations were made which are worth reporting for they may help to shed some light on

future studies. These are:

1. All whirl was translatory at onset with unequal amplitudes on the dummy and turbine ends. The turbine end ran generally smaller in amplitude than the dummy end, however, within the region of half frequency whirl a change was noted in whirl pattern as the speed increased. At a certain point the amplitude at the turbine end would become larger and the whirl would change from translatory to conical. Scope traces of this condition are shown in Figs. 16-17, for bearing of L/D ratio of 2.

2. The growth of amplitude as function of speed within the half frequency whirl region is more violent with:
   a. High clearance bearings
   b. L/D of 1 rather than 2
   c. High load
   d. Large mass or inertia

   (It is interesting to note that with L/D of 2 and radial clearance of 0.000611", the inherently unstable aluminum rotor with 4.01 lbs. per bearing could be safely operated within the region of half frequency whirl up to 14,000 RPM, at the same time the steel rotor, inclined to yield the same bearing load, also inherently unstable, could only be operated up to 4,000 RPM before physical contact between rotor and bearing was established.)

3. Once a rotor becomes unstable the instability persists during decelleration or coast down, to a speed lower than that of the onset. (This phenomena can be considered as "hysteresis of instability".) As soon, however, as the original onset speed has been left behind, a sharp, sudden blow will restore stability.

4. For all tests the ratio of whirl frequency to shaft rotational frequency was between 0.480 and 0.495.

E. Test Results - L/D = 1

The test results for L/D ratio of 1, diameter of 2.00 inch and variable loading from 11.01 to 4.02 lbs. per bearing at constant mass and inertia are given in tables 13-15. The load variation was accomplished through housing inclination. Onset speeds are given for 0^{o} and 180^{o} positions with open and plugged orifice.

It can be seen that orifice plugging reduces the difference in onset speeds between the 0^{o} and 180^{o} position, but in no case makes the two identical. It is suspected that effectiveness of sealing arrangement as well as dead ended hole introduced in the bearing may be responsible for the indicated differences. Values of initial disturbance lower than "actual onset" are given in parenthesis.

Table 16 summarizes the data of tables 13-15 for the orifice open and in the 0^{o} position. It also includes dimensionless load and compressibility numbers, as well as calculated values of eccentricity ratio and attitude angle. To the best of our knowledge this is the first time that onsets of instability have been recorded at high eccentricity ratios. In general, it was thought that instability occurs only in lightly loaded bearings, i.e., only in rotors operating at low eccentricity ratios.

Table 17 presents data for the same bearing geometries as table 16, but with orifice open and in 180^{o} position. The pronounced effect of orifice location can be seen by comparison of table 16 and 17. The influence of orifice on stability was found to be most pronounced in the 150^{o}-210^{o} region. For more details see Ref. 5. Similar effects have been

observed by investigators in the past with intentionally slotted bearings (Refs. 5, 6, 7). The vent produced by the orifice has a tendency to partially destroying the lower than ambient pressure region, thus altering the pressure distribution in a way which produces a net effect of increase in onset of HFW. The difference between onset speeds in 0^{o} and 180^{o} positions seems to be decreasing as the clearance increases probably due to increased eccentricity ratio and reduced lower than ambient pressures in the suction areas.

The experimental data indicates that the threshold of instability is a function of rotor mass, bearing load and clearance. With this bearing L/D ratio only three clearances were evaluated. Curves of the onset of HFW vs. clearance for various loads are shown in Fig. 18. Note that a bearing clearance exists which gives minimum speed for the onset of instability. On either side of this clearance the onset speed is greater.

Fig. 19 was plotted from data obtained in this study and that obtained from Ref. 7. Several important conclusions can be drawn from this figure and Fig. 21.

1. The onset of HFW increases almost linearly with load. (This leads to the conclusion that $\Lambda/W \approx$ constant.)
2. The onset of cylindrical HFW increases with increase in rotor mass.
3. The onset of HFW is zero when $M/W = \infty$. (This corresponds to the case of vertical rotor $W = 0$.)

Referring to tables 16 and 17 two additional important conclusions may be drawn which indicate that:

1. For a given rotor mass and bearing clearance the eccentricity ratio at the onset of instability remains virtually constant even thought the bearing load is varied.

2. As the bearing clearance increases so does the eccentricity ratio at onset of instability.

F. Test Results - L/D = 2

This data is presented in similar manner to that for L/D = 1. Tables 18-22 show effects of load on onset of half frequency whirl for three different clearances. Wherever values are lacking, same have not been reported due to poor repeatability which in most cases was traced to poor bearing condition due to frequent rubbing within the region of half frequency whirl.

Tables 23 and 24 show calculated values of eccentricity ratio and attitude angle based on analytical results presented in Ref. 1.

The onset of half frequency whirl as function of bearing clearance is shown in Figs. 20a and 20b. The results plotted in Fig. 20a represent the actual onset of HFW for the plugged orifice in 180° position while Fig. 20b represents the initial disturbance for the orifice open in 0° position. For this orifice position the initial disturbance and the actual onset speed do not coincide only for bearings with 0.000771" and 0.00122" clearance. Comparison of these two figures shows the range of speeds between the initial disturbance and actual onset. Since within this region the instability may be in the small it may be difficult to detect and may have been missed experimentally by various investigators. It is believed that the data presented in Ref. 7 is for onset of half frequency whirl rather than initial disturbance. Both of these figures, however, indicate the same trends with a minimum speed of half frequency whirl which seems to occur within radial clearance of 0.00075" - 0.0011".

Decreases as well as increases from this clearance range will increase the speed at which half frequency whirl sets in, the decrease in clearance being much more effective than increase as the slopes seem to indicate.

Fig. 21 shows the effect of bearing load on the onset of HFW. This figure like Fig. 19 was obtained from the data obtained in this program and that presented in Ref. 7. The same conclusions as stated previously apply.

Fig. 22 shows comparison between theory and experiment for the initial disturbance as a function of bearing clearance for L/D = 2 and b = 1.0. This clearly indicates the existence of minimum frequency for initial disturbance. The comparison is very good for other values of b. See Ref. 3. Unfortunately the data for L/D = 2 presented in Ref. 7 and plotted in Fig. 21 was for C = 0.0008" while that for L/D = 1 was for C = 0.0006", thus direct comparison of the effect of L/D ratio on the onset of instability is difficult. For this reason Fig. 23 was plotted which shows the effect of L/D on the onset of half frequency whirl. Three important conclusions may be drawn from this figure:

1. The higher the ratio of p/p_a the higher the onset of HFW.
2. For the same value of p/p_a the higher the L/D ratio the lower the onset of HFW.
3. For the same bearing load the higher the L/D ratio the lower the onset of HFW.

CONCLUSIONS

1.) There is good agreement between theory and experiment for static load carrying capacity, eccentricity ratio and attitude angle for plain cylindrical journal bearings.

2.) There is a clearance which gives minimum onset speed for a given bearing load. On either side of this clearance the threshold of HFW is greater.

3.) The onset of HFW increases almost linearly with load. (This leads to the conclusion that $\Lambda/W \approx$ constant.)

4.) The onset of cylindrical HFW increases with increase in rotor mass.

5.) The onset of HFW is zero when $M/W = \infty$. (This corresponds to the case of vertical rotor W = 0.)

6.) For a given rotor mass and bearing clearance the eccentricity ratio at the onset of instability remains virtually constant even though the bearing load is varied significantly.

7.) As the bearing clearance increases so does the eccentricity ratio at onset of instability.

8.) For the same value of p/p_a the higher the L/D ratio the lower the onset of HFW.

9.) Frequency of initial disturbance may not coincide with the onset of half frequency whirl. In this region the instability is in the small and any external forces tend to damp out large amplitude oscillations.

10.) Magnitude of angle between a small orifice vented to atmosphere and the load vector will markedly influence the onset of HFW.

11.) The growth of amplitude as function of speed within the half frequency whirl region is more violent with:

a.) High clearance bearings

b.) L/D of 1 rather than 2

c.) High load

d.) Large mass or inertia

ACKNOWLEDGMENT

We wish to thank Mr. G.J. Kaloust who consulted on instrumentation and Messrs. J. Devikis and R. Dow who assisted in obtaining the test data.

REFERENCES

1. B. Sternlicht, H. Poritsky and E. Arwas, "Dynamic Stability Aspects of Cylindrical Journal Bearings using Compressible and Incompressible Fluids", Proceedings, First International Gas Bearing Symposium, Sponsored by ONR, Washington, D.C., 1959.

2. B. Sternlicht, "Gas Lubricated Cylindrical Journal Bearings of Finite Length", Part I - Static Loading. Technical Report for Office of Naval Research, Contract No. 2844(00), Task No., NR097-348, August 15, 1960.

3. G.M. Rentzepis and B. Sternlicht, "On the Stability of Rotors in Cylindrical Journal Bearings", Technical Report for ONR, Contract No. NONR 2844(00), Task No. NR097-348, May 15, 1961.

4. R.C. Elwell, R.J. Hooker, B. Sternlicht, "Gas Bearing Stability Study - Vertical Rotor Investigation", Technical Report for ONR, Contract No. NONR 2844(00), Task No. NR097-348.

5. B. Sternlicht and L.W. Winn, "Geometry Effects on Threshold of Half Frequency Whirl in Gas Journal Bearings", ONR Report.

6. S. Whitley and C. Betts, "A Study of Gas Lubricated, Hydrodynamic, Full Journal Bearings", United Kingdom Atomic Energy Authority, Industrial Group Report No. 20(RD/CA), 1959.

7. S. Whitley, A.J. Bowhill and P. McEwan, "The Load Capacity and Half-Speed Whirl of Hydrodynamic Gas Journal Bearings", UKAEA Report DEG 199(CA), 1960.

LIST OF TABLES

TABLE NO. 1

Test No. 1

RPM	ω rad/sec	Λ	f	ϵ	ϕ
750	78.54	.2318	15.226	.46	86
1500	157.08	.4637	7.612	.29	74
3000	314.16	.9274	3.806	.13	58
4000	418.88	1.2365	2.854	.09	49

$\mu = 2.7\ (10^{-9})$ lb.sec/in.^{2} L = 4" C = 0.000611"

p_a = 14.7 psia R = 1" F = 11.01 lb.

TABLE NO. 2

Test No. 1A

RPM	ω rad/sec	Λ	f	ϵ	ϕ
1000	104.72	.3091	9.894	.33	78
2000	209.44	.6183	4.946	.17	67
3000	314.16	.9274	3.298	.13	57

$\mu = 2.7\ (10^{-9})$ lb.sec/in.^{2} L = 4" C = 0.000611"

p_a = 14.7 psia R = 1" F = 9.54 lb.

TABLE NO. 3

Test No. 1B

RPM	ω rad/sec	Λ	f	ϵ	ϕ
1000	104.72	.3091	8.069	.28	75
2000	209.44	.6183	4.034	.14	60

$\mu = 2.7\ (10^{-9})$ lb.sec/in.^{2} L = 4" C = 0.000611"

p_a = 14.7 psia R = 1" F = 7.78 lb.

TABLE NO. 4

Test No. 2

RPM	ω rad/sec	Λ	f	ϵ	ϕ
1000	104.72	.1145	30.825	.76	76
2000	209.44	.2290	15.413	.49	76
3000	314.16	.3435	10.275	.34	76.5

$\mu = 2.7\ (10^{-9})$ lb.sec/in.^{2} L = 4" C = 0.001004"

p_a = 14.7 R = 1" F = 11.01 lb.

TABLE NO. 5

Test No. 2A

RPM	ω rad/sec	Λ	f	ϵ	ϕ
1000	104.72	.1145	26.710	.63	80
2000	209.44	.2290	13.355	.41	78
3000	314.16	.3435	8.903	.31	74

$\mu = 2.7\ (10^{-9})$ lb.sec/in.^{2} L = 4" C = 0.001004"

p_a = 14.7 psia R = 1" F = 9.54 lb.

TABLE NO. 6

Test No. 2B

RPM	ω rad/sec	Λ	f	ϵ	ϕ
1000	104.72	.1145	21.782	.54	81

$\mu = 2.7\ (10^{-9})$ lb.sec/in.^{2} L = 4" C = 0.001004"

p_a = 14.7 psia R = 1" F = 7.78 lb.

TABLE NO. 7

Test No. 3

RPM	ω rad/sec	Λ	f	ϵ	ϕ
1000	104.72	.3091	22.837	.75	50
2000	209.44	.6183	11.417	.57	66
3000	314.16	.9274	7.612	.47	69
4000	418.88	1.237	5.707	.39	72
5000	523.6	1.546	4.566	.32	75
6000	628.32	1.855	3.805	.30	64
7000	733.04	2.1640	3.262	.29	50

$\mu = 2.7\ (10^{-9})$ lb.sec/in.^{2} L = 2" C = 0.000611"

p_a = 14.7 psia R = 1" F = 11.01 lb.

TABLE NO. 8

Test No. 3A

RPM	ω rad/sec	Λ	f	ϵ	ϕ
1000	104.72	.3091	16.137	.69	60
2000	209.44	.6183	8.067	.45	73
3000	314.16	.9274	5.379	.34	68
4000	418.88	1.237	4.032	.28	67
5000	523.6	1.546	3.226	.23	62

$\mu = 2.7\ (10^{-9})$ lb.sec/in.^{2} L = 2" C = 0.000611"

p_a = 14.7 psia R = 1" F = 7.78 lb.

TABLE NO. 9

Test No. 3B

RPM	ω rad/sec	Λ	f	ϵ	ϕ
1000	104.72	.3091	8.338	.51	73
2000	209.44	.6183	4.169	.32	74
3000	314.16	.9274	2.779	.23	72

$\mu = 2.7\ (10^{-9})$ lb.sec/in.^{2} L = 2" C = 0.000611"

p_a = 14.7 psia R = 1" F = 4.02 lb.

TABLE NO. 10

Test No. 4

RPM	ω rad/sec	Λ	f	ϵ	ϕ
2000	209.44	.1742	40.5	.82	54
3000	314.16	.261	26.98	.77	61
4000	418.88	.349	20.02	.73	64
5000	523.6	.436	16.15	.68	67
6000	628.32	.522	13.50	.64	72
7000	733.04	.610	11.60	.60	73

$\mu = 2.7\ (10^{-9})$ lb.sec/in.^{2} L = 2" C = 0.001147"

p_a = 14.7 psia R = 1" F = 11.01 lb.

TABLE NO. 11

Test No. 4A

RPM	ω rad/sec	Λ	f	ϵ	ϕ
2000	209.44	.1742	28.6	.77	64
3000	314.16	.261	18.82	.71	68
4000	418.88	.349	14.31	.64	71
5000	523.6	.436	11.46	.60	73
6000	628.32	.522	9.42	.54	75

$\mu = 2.7\ (10^{-9})$ lb.sec/in.^{2} L = 2" C = .001147"

p_a = 14.7 psia R = 1" F = 7.78 lb.

TABLE NO. 12

Test No. 4B

RPM	ω rad/sec	Λ	f	ϵ	ϕ
1000	104.72	.0875	30.9	.80	67
2000	209.44	.1742	15.46	.66	77
3000	314.16	.261	10.28	.54	81

$\mu = 2.7\ (10^{-9})$ lb.sec/in.^{2} L = 2" C = .001147"

p_a = 14.7 psia R = 1" F = 4.02 lb.

TABLE NO. 13

HFW

L/D = 1 D = 2" C = 0.000611" $\mu = 2.7 \times 10^{-9}$ lb.sec/in.^{2}

STEEL ROTOR $p_a = 14.7$ psia

Brg. Load lb.	Onset of HFW - RPM 0° Pos. Orifice Open	Orifice Plugged	Onset of HFW - RPM 180° Pos. Orifice Open	Orifice Plugged
11.01	7470	7800	11,200	9120
10.62	7400		11,130	
9.54	7000		10,820	
7.78	5940		9,620	
5.50	4450	4870	7,170	5770
4.02	3380		5,220	

ALUMINUM ROTOR

4.02	5300 (Starts at 3460)	6320	8,310	7140

TABLE NO. 14

HFW

L/D = 1 D = 2" C = 0.001147" $\mu = 2.7 \times 10^{-9}$ lb.sec/in.^{2}

STEEL ROTOR

$p_a = 14.7$ psia

Brg. Load lb.	Onset of HFW - RPM 0° Pos. Orifice Open	Onset of HFW - RPM 0° Pos. Orifice Plugged	Onset of HFW - RPM 180° Pos. Orifice Open	Onset of HFW - RPM 180° Pos. Orifice Plugged
11.01	9300	9310	12,320	10,220
10.62	9110	9100	9,890	9,500
9.54	8290	8430	9,890	9,340
7.78	7010	7490	8,250	8,050
5.50	4950	5500	5,850	5,620
4.02	3300	3490	4,660	3,550

ALUMINUM ROTOR

4.02	5000 (Starts at 3800)			

TABLE NO. 15

HFW

L/D = 1 D = 2" C = 0.001643" $\mu = 2.7 \times 10^{-9}$ lb.sec/in.^{2}

STEEL ROTOR $p_a = 14.7$ psia

Brg. Load lb.	Onset of HFW - RPM 0° Pos. Orifice Open	Onset of HFW - RPM 0° Pos. Orifice Plugged	Onset of HFW - RPM 180° Pos. Orifice Open	Onset of HFW - RPM 180° Pos. Orifice Plugged
11.01	9580	10,420	11,900	11,800
10.62	9540	10,310	11,300	11,170
9.54	8820	9,650	10,660	10,470
7.78	7410	8,470	8,770	8,510
5.50	5400	6,000	6,120	6,020
4.01	3780 (Starts at 3300)	3,800	4,300 (Starts at 3300)	4,010

ALUMINUM ROTOR

4.02	4060 (Starts at 3600)	5,300	6,080	6,050

TABLE NO. 16

Half Frequency Whirl Data

Steel Rotor - L/D = 1

0^{o} Position - Open Orifice

Test No.	C in.	F lb.	f	Λ	N RPM	ϵ	ϕ
10	0.000611	11.01	3.062	2.315	7,470	.25	53
		10.62	2.970	2.290	7,400	.25	54
		9.54	2.840	2.170	7,000	.24	54
		7.78	2.720	1.850	5,940	.23	56
		5.50	2.670	1.380	4,450	.21	62
		4.02	2.470	1.050	3,380	.20	68
11	0.001147	11.01	9.02	.810	9,300	.51	65
		10.62	8.87	.792	9,110	.50	66
		9.54	8.76	.722	8,290	.49	68
		7.78	8.45	.610	7,010	.48	71
		5.50	8.45	.431	4,950	.48	76
		4.02	9.30	.287	3,300	.50	80
12	0.001643	11.01	17.30	.409	9,580	.70	61
		10.62	16.70	.407	9,540	.69	62
		9.54	16.20	.376	8,820	.68	63
		7.78	15.70	.317	7,410	.67	68
		5.50	15.20	.231	5,400	.66	76
		4.02	15.90	.162	3,300	.67	80

TABLE NO. 17

Half Frequency Whirl Data
Steel Rotor - 180° Position
L/D = 1 - Open Orifice

Test No.	C in.	F lb.	f	Λ	N RPM	ϵ	ϕ
10	.000611	11.01	2.04	3.47	11,200	.21	52
		10.62	1.97	3.44	11,130	.19*	54
		9.54	1.84	3.35	10,820	.20	55
		7.78	1.68	2.98	9,620	.19*	59
		5.50	1.66	2.22	7,170	.18*	67
		4.02	1.60	1.61	5,220	.16*	71
11	.001147	11.01	6.80	1.07	11,850	.43	68
		10.62	8.16	.862	11,000	.47	66
		9.54	7.45	.862	9,890	.45	68
		7.78	7.19	.718	8,250	.43	72
		5.50	7.16	.510	5,850	.43	77
		4.02	6.59	.406	4,660	.40	81
12	.001643	11.01	15.00	.507	11,900	.64	63
		10.62	15.00	.484	11,300	.64	63
		9.54	13.40	.455	10,660	.62	66
		7.78	13.3	.375	8,770	.61	70
		5.50	13.5	.261	6,120	.61	76
		4.02	14.0	.184	4,300	.63	80

*Extrapolated

TABLE NO. 18

HFW

L/D = 2 D = 2" C = .000445" $\mu = 2.7 \times 10^{-9}$ lb.sec/in.^{2}

Steel Rotor p_a = 14.7 psia

Brg. Load lb.	Onset of HFW - RPM 0° Pos.		Onset of HFW - RPM 180° Pos.	
	Orifice Open	Orifice Plugged	Orifice Open	Orifice Plugged
11.01	8260	8990	9380	9160
10.62	8000	8700	9100	8580
9.54	7200	8470	8700	8140
7.78	6000	7190	7850	7370
5.50	5040	5470	7000	6130
4.01	3870	5390	5970	5260

TABLE NO. 19

HFW

L/D = 2 D = 2" C = 0.000611" $\mu = 2.7 \times 10^{-9}$ lb.sec/in.^{2}

Steel Rotor $p_a = 14.7$ psia

Brg. Load lb.	Onset of HFW - RPM 0° Pos.		Onset of HFW - RPM 180° Pos.	
	Orifice Open	Orifice Plugged	Orifice Open	Orifice Plugged
11.01	4100		7700	
10.62	3970		7220	
9.54	3210		6880	
7.78	2370		4000	

TABLE NO. 20

HFW

L/D = 2 D = 2" C = 0.000771" $\mu = 2.7 \times 10^{-9}$ lb.sec/in.^{2}

Steel Rotor $p_a = 14.7$ psia

Brg. Load lb.	Onset of HFW - RPM 0° Pos.		Onset of HFW - RPM 180° Pos.	
	Orifice Open	Orifice Plugged	Orifice Open	Orifice Plugged
11.01	4280 (3200)*	5480 (3240)	7130	6600
10.62	4230 (3190)	5350 (3200)	6910	6420
9.54	3340 (2450)	4860 (2850)	6140	5620
7.78	3200 (1260)	4000 (1900)	4760	4010
5.50	1660 (Low)	2500 (Low)	3410	3400

*Values in parenthesis indicate speed at which initial disturbance occurs, other values denote speed at which the amplitude of HFW mushrooms out with slight increase in speed.

TABLE NO. 21

HFW

L/D = 2 D = 2" C = 0.001003" $\mu = 2.7 \times 10^{-9}$ lb.sec/in.^{2}

Steel Rotor $p_a = 14.7$ psia

Brg. Load lb.	Onset of HFW - RPM 0^o Pos.		Onset of HFW - RPM 180^o Pos.	
	Orifice Open	Orifice Plugged	Orifice Open	Orifice Plugged
11.01	3260		6600	
10.62	3170		6420	
9.54	3160		5480	
7.78	1810		3610	

TABLE NO. 22

HFW

$L/D = 2$ $D = 2"$ $C = .00122"$ $\mu = 2.7 \times 10^{-9}$ lb.sec/in.^{2}

Steel Rotor $p_a = 14.7$ psia

Brg. Load lb.	Onset of HFW - RPM 0^o Pos.		Onset of HFW - RPM 180^o Pos.	
	Orifice Open	Orifice Plugged	Orifice Open	Orifice Plugged
11.01	4560 (3500)*	5580 (3700)	6310	5980
10.62	4140 (3370)	5420 (3520)	6180	5750
9.54	3650 (3070)	4900 (3200)	5560	5130
7.78	2960 (2140)	4260 (2300)	4860	4360
5.50	2100 (1700)	3140 (1700)	3300	3200

*Values in parenthesis indicate speed at which initial disturbance occurs, other values denote speed at which the amplitude of HFW mushrooms out with slight increase in speed.

TABLE NO. 23

Half Frequency Whirl Data
Steel Rotor - L/D = 2
0^{o} Position - Open Orifice

Test No.	C in.	F lb.	f	Λ	N RPM	ϵ	ϕ
5	.000445	11.01	0.734	4.812	8,260	.07	23
		10.62	0.731	4.660	8,000	.07	22
		9.54	0.730	4.192	7,200	.06	25
		7.78	0.713	3.496	6,000	.05	30
		5.50	0.600	2.936	5,040	.04*	36*
		4.02	0.572	2.254	3,870	.03*	45*
6	.000611	11.01	2.78	1.27	4,100	.12*	52
		10.62	2.76	1.23	3,970	.13*	53
		9.54	3.08	1.00	3,210	.14*	59
		7.78	3.28	0.732	2,370	.15*	66
		5.50	6.40	0.276	890	.18*	80
7	.000771	11.01	5.68	0.621	3,200	.19	70
		10.62	5.50	0.619	3,190	.19	70
		9.54	6.42	0.476	2,450	.21	72
		7.78	10.18	0.245	1,260	.32	79
		5.50	10.08	0.175	900	.32	82
8	.001003	11.01	9.45	0.374	3,260	.30	75
		10.62	9.37	0.363	3,170	.30	76
		9.54	8.35	0.362	3,160	.28	77
		7.78	12.01	0.208	1,810	.35	81
		5.50	17.10	0.103	900	.45	84
9	.001220	11.01	13.02	0.271	3,500	.40	78
		10.62	13.04	0.261	3,370	.40	78
		9.54	12.85	0.238	3,070	.39	79
		7.78	15.02	0.166	2,140	.44	81
		5.50	13.36	0.132	1,700(?)	.40	84

*Extrapolated

TABLE NO. 24

Half Frequency Whirl Data
Steel Rotor - L/D = 2
0^{o} Position - Open Orifice

Test No.	C in.	F lb.	f	Λ	N RPM	ϵ	ϕ
5	.000445	11.01	0.646	5.465	9,380	.07	20
		10.62	0.642	5.304	9,100	.07	20
		9.54	0.603	5.072	8,700	.06	21
		7.78	0.545	4.576	7,850	.05	24
		5.50	0.432	4.080	7,000	.04*	27*
		4.02	0.370	3.480	5,970	.03*	33*
6	.000611	11.02	1.48	2.38	7,700	.09	37
		10.62	1.57	2.24	7,220	.09	38
		9.54	1.43	2.13	6,880	.08	40
		7.78	1.95	1.24	4,000	.08	56
7	.000771	11.01	2.55	1.385	7,130	.11	50
		10.62	2.54	1.342	6,910	.11	51
		9.54	2.56	1.192	6,140	.11	54
		7.78	2.70	0.924	4,760	.10	61
		5.50	2.66	0.662	3,410	.09	69
8	.001003	11.01	4.67	.756	6,600	.16	65
		10.62	4.64	.735	6,420	.16	66
		9.54	4.82	.628	5,480	.16	68
		7.78	6.03	.356	3,610	.19	77
9	.001220	11.01	7.22	.489	6,310	.24	72
		10.62	7.09	.480	6,180	.24	72
		9.54	7.11	.430	5,560	.23	74
		7.78	6.62	.377	4,860	.22	76
*Extrapolated		5.50	6.89	.256	3,300	.22	80

LIST OF FIGURES

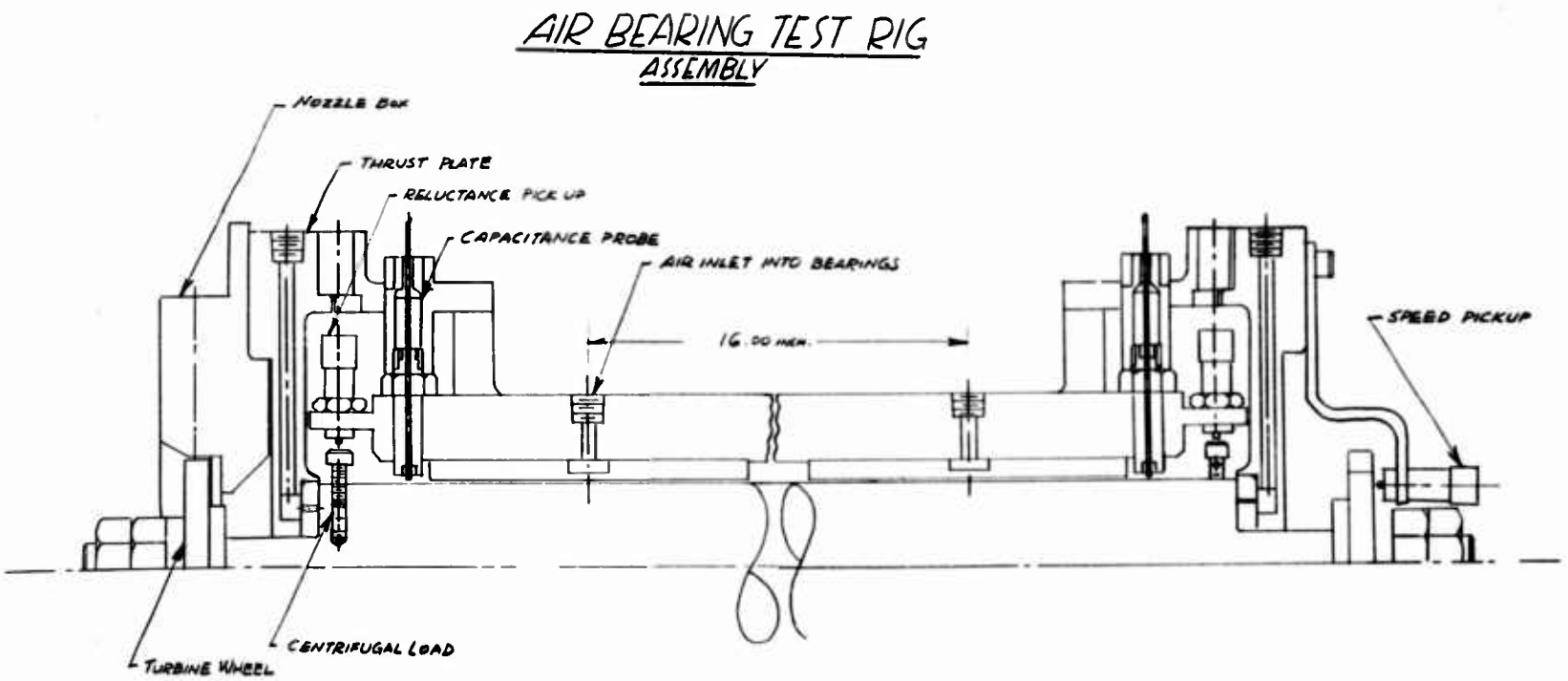

Fig. 1. Test rig drawing.

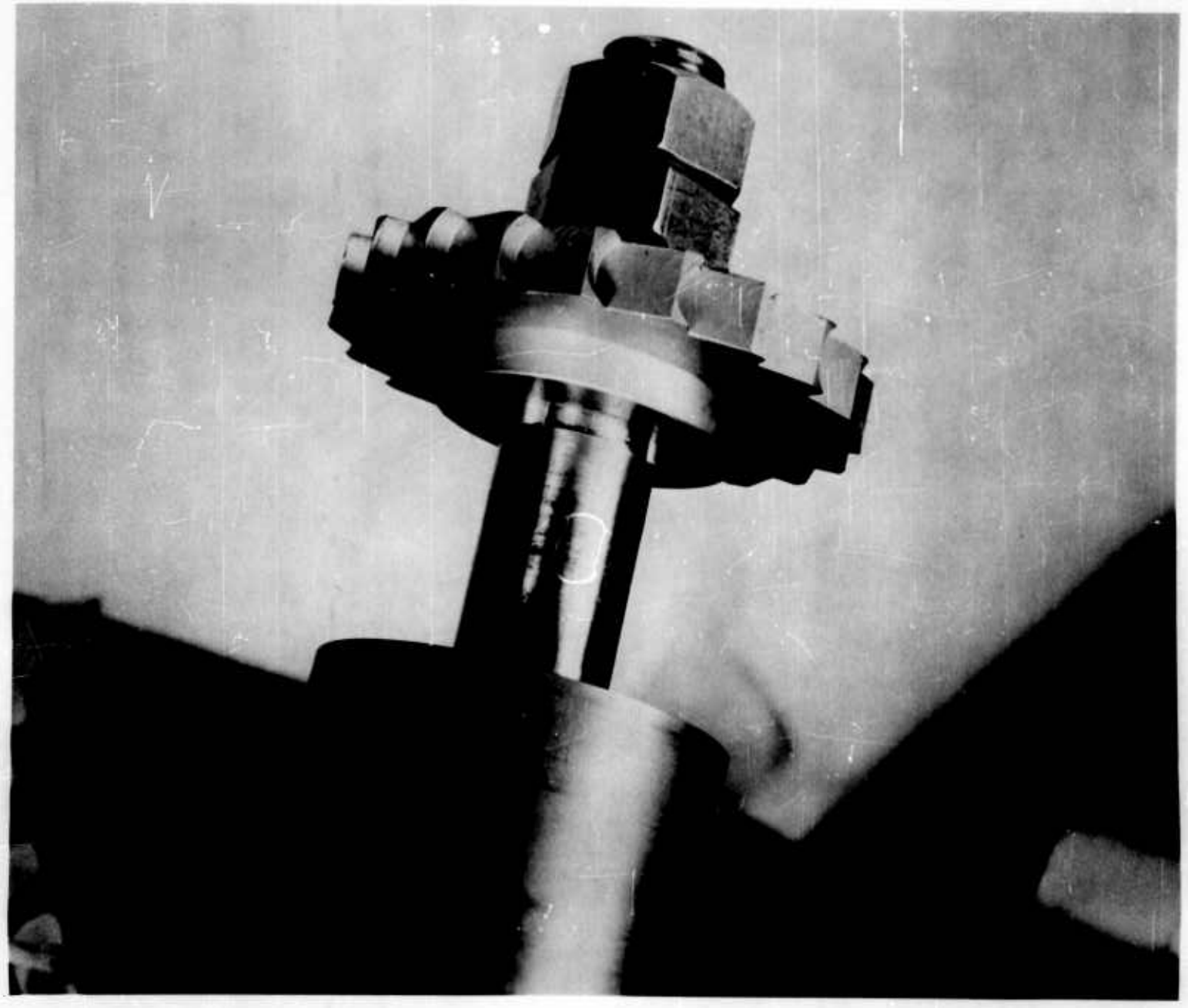

Fig. 2. Turbine wheel locking arrangement showing woodroof keys and locknuts.

THRUST PLATE

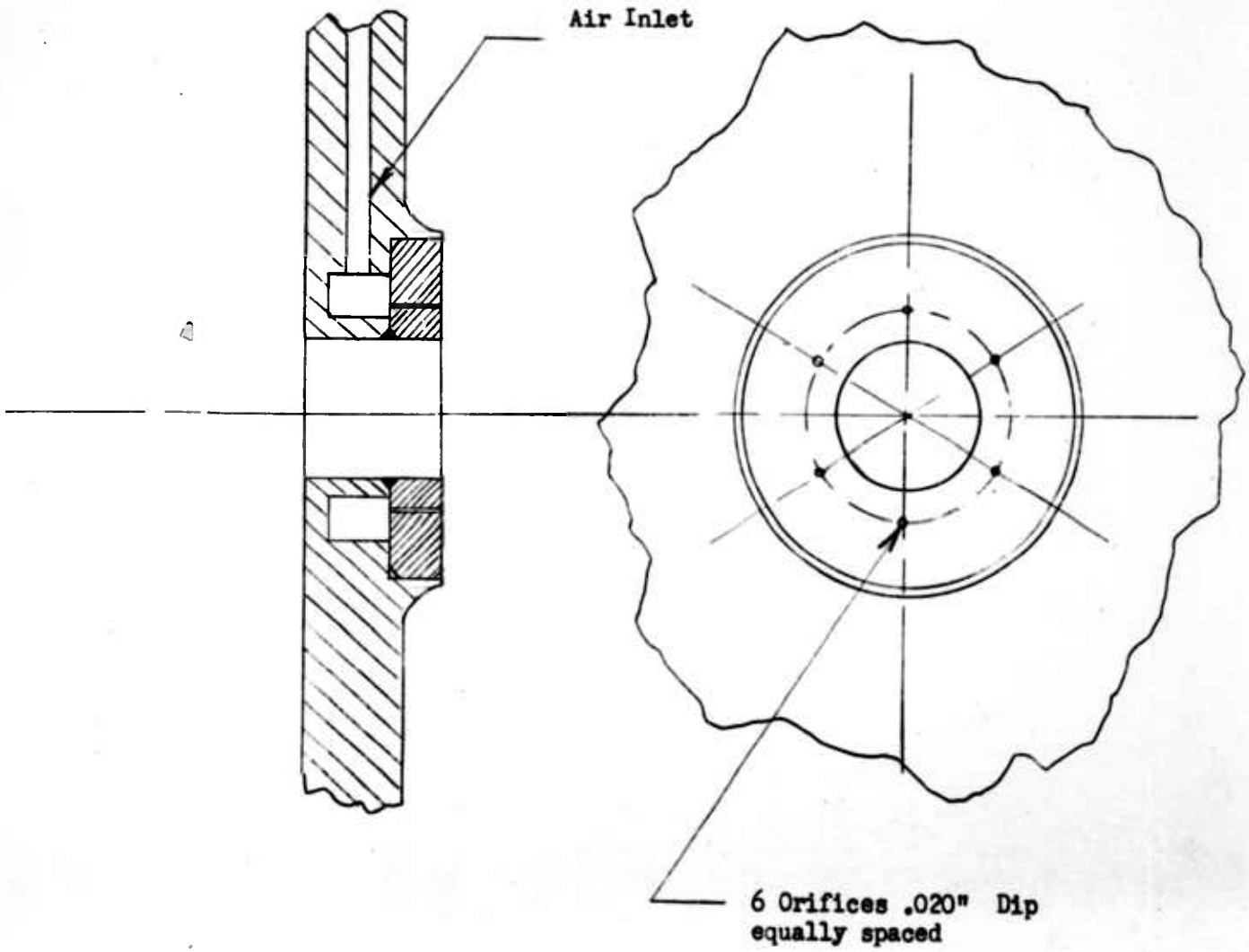

Fig. 3. Thrust plate drawing.

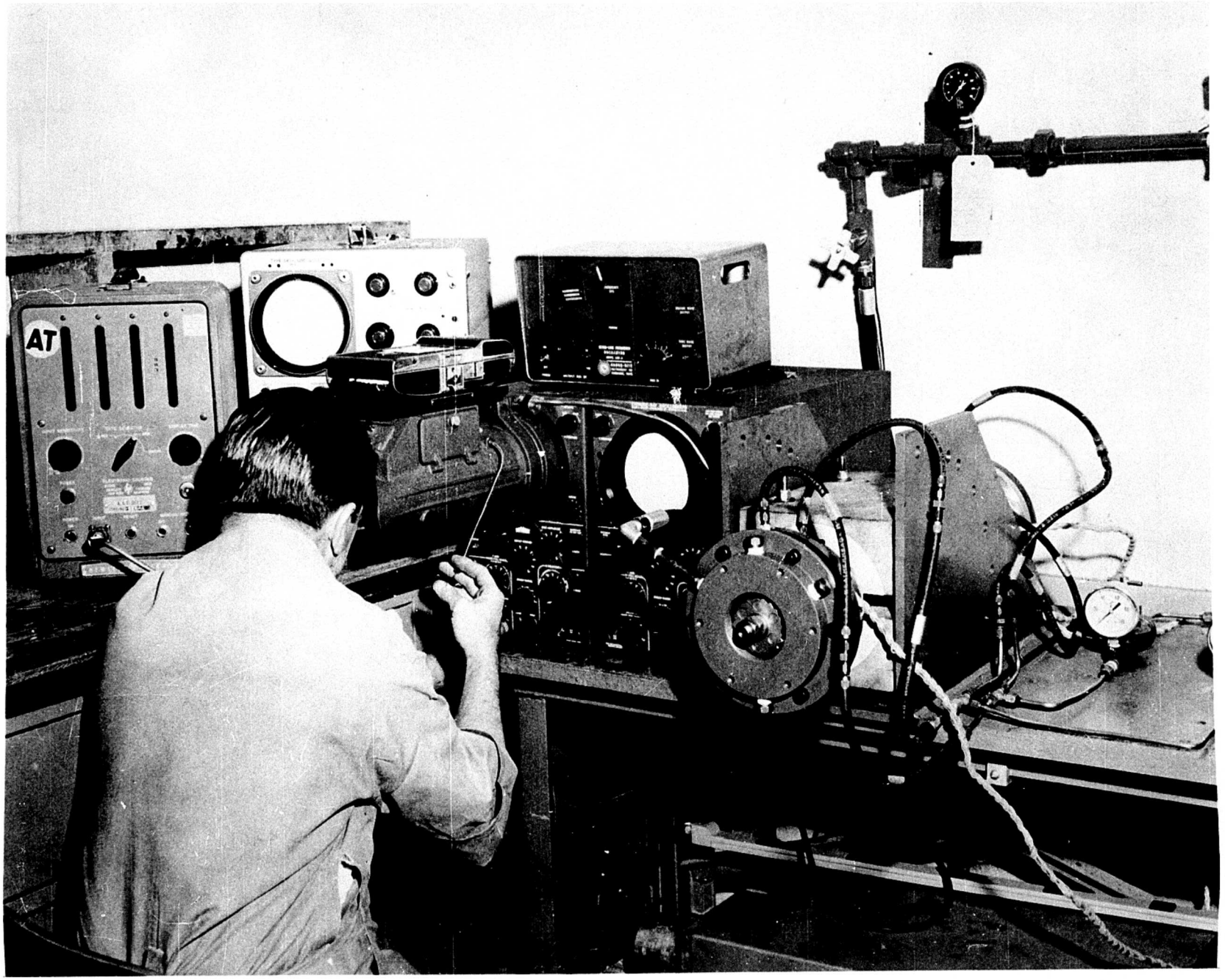

Fig. 4. General test set up.

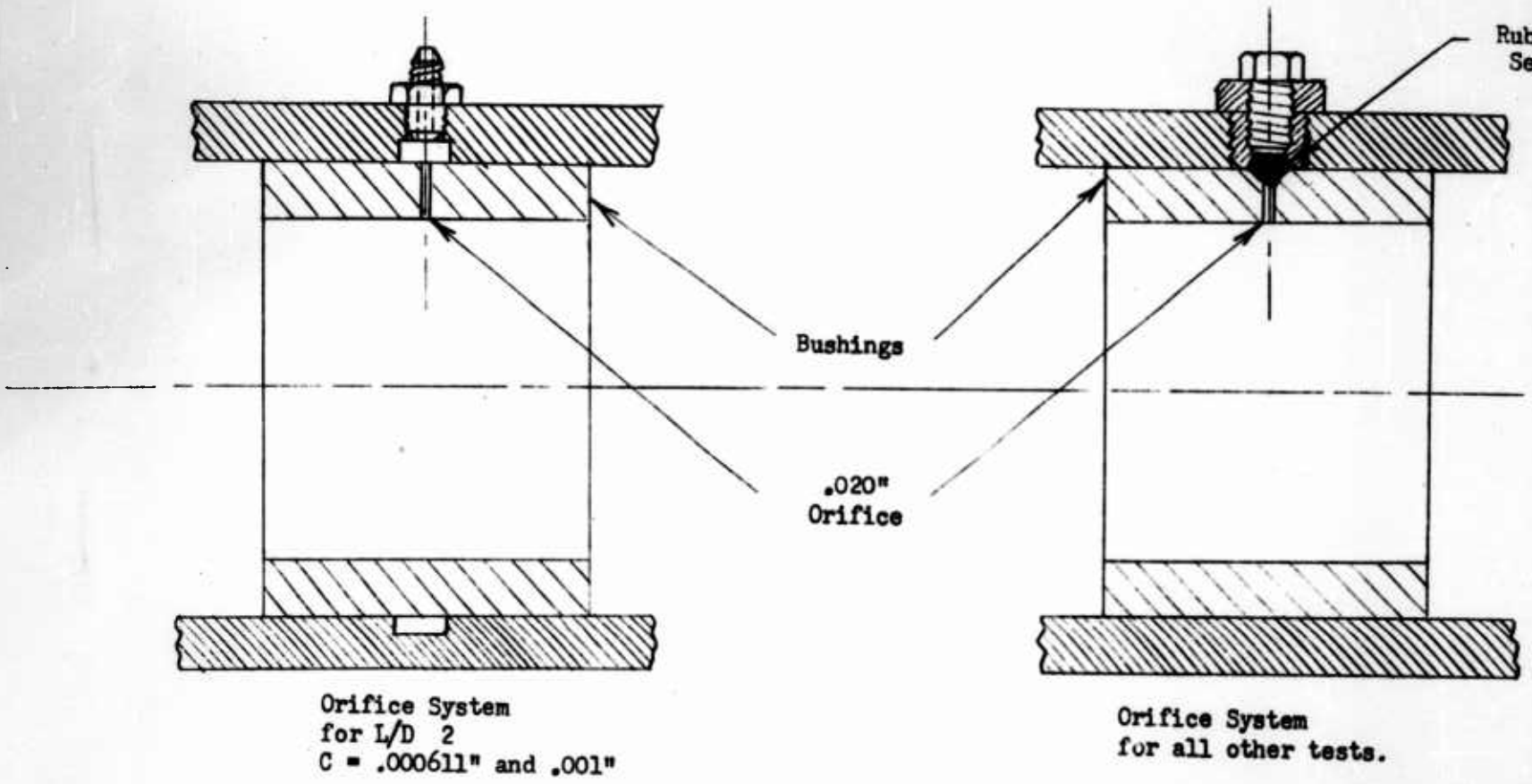

Fig. 5. Plugging arrangement for orifice.

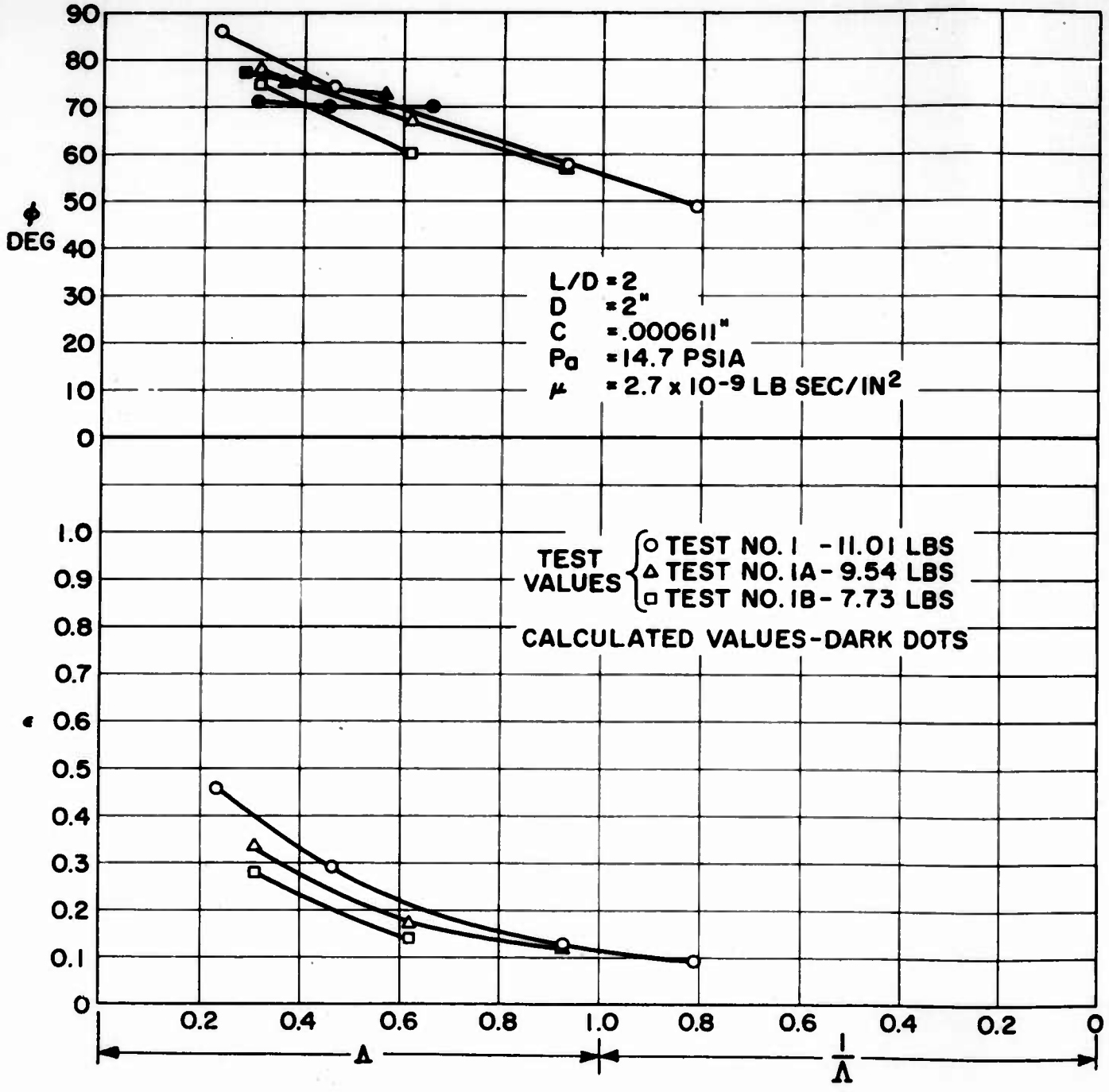

Fig. 6. Plots of Ø and ε vs.

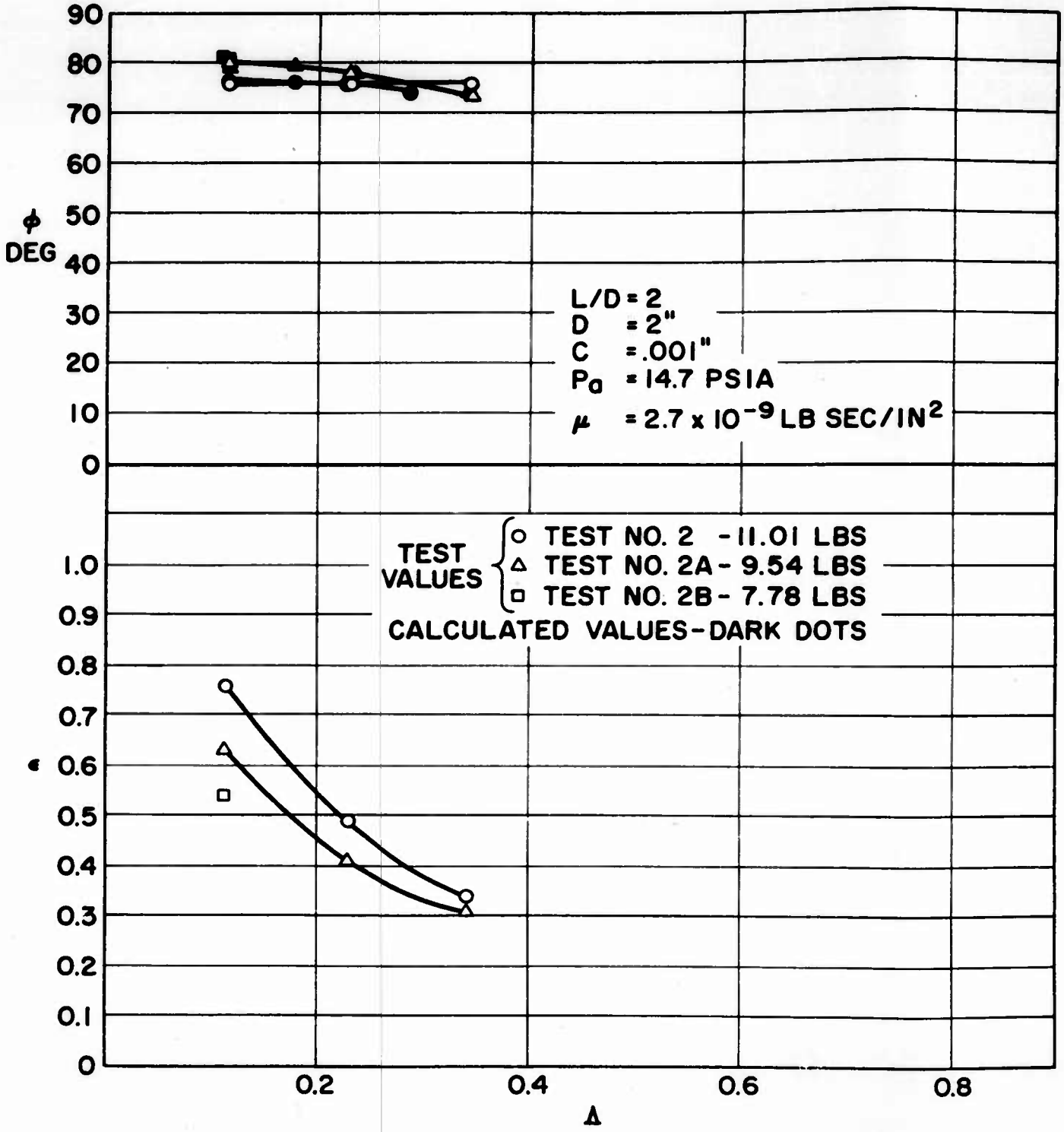

Fig. 7. Plots of ϕ and ε vs. Λ

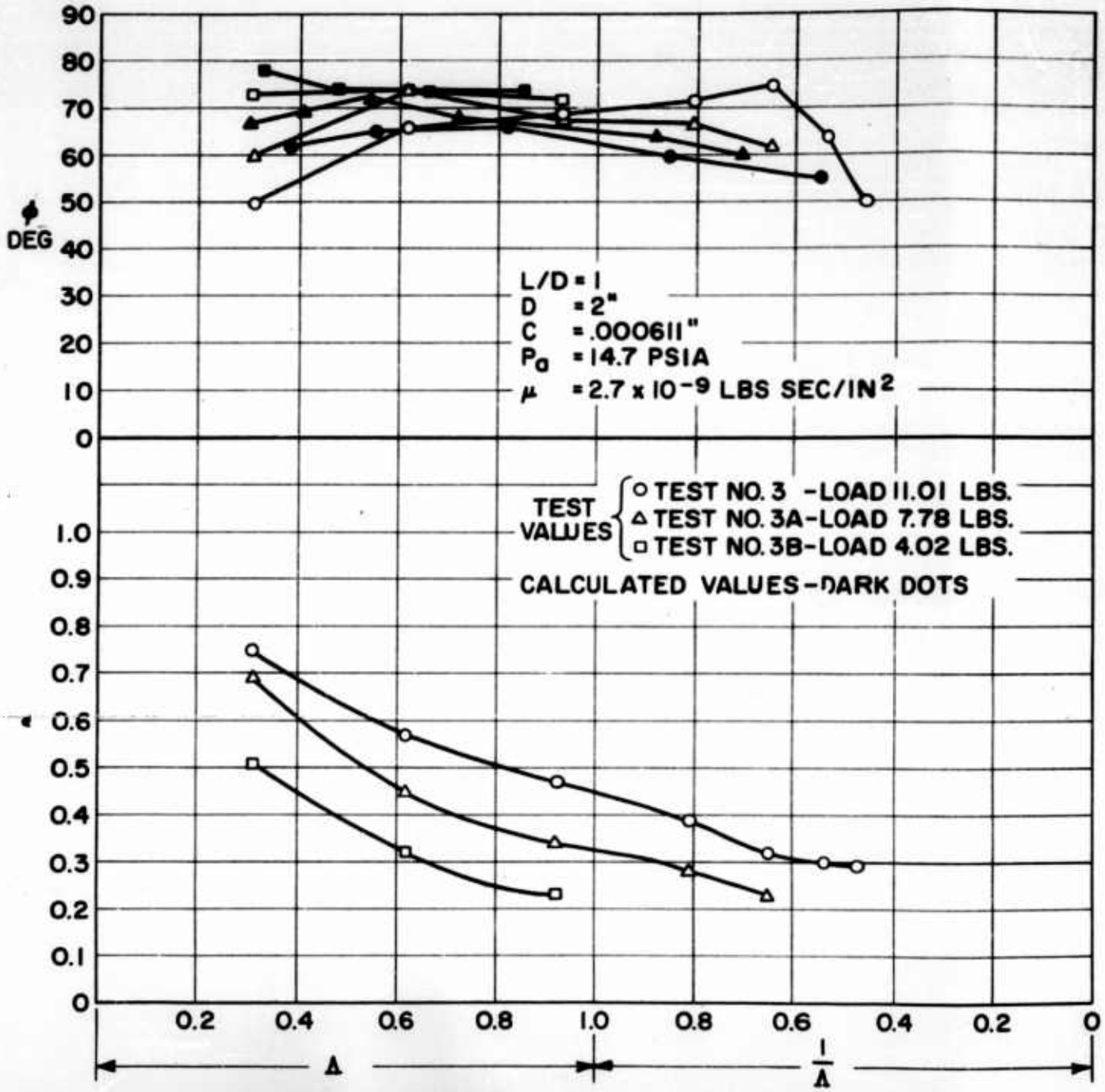

Fig. 8. Plots of ϕ and ε vs. Λ.

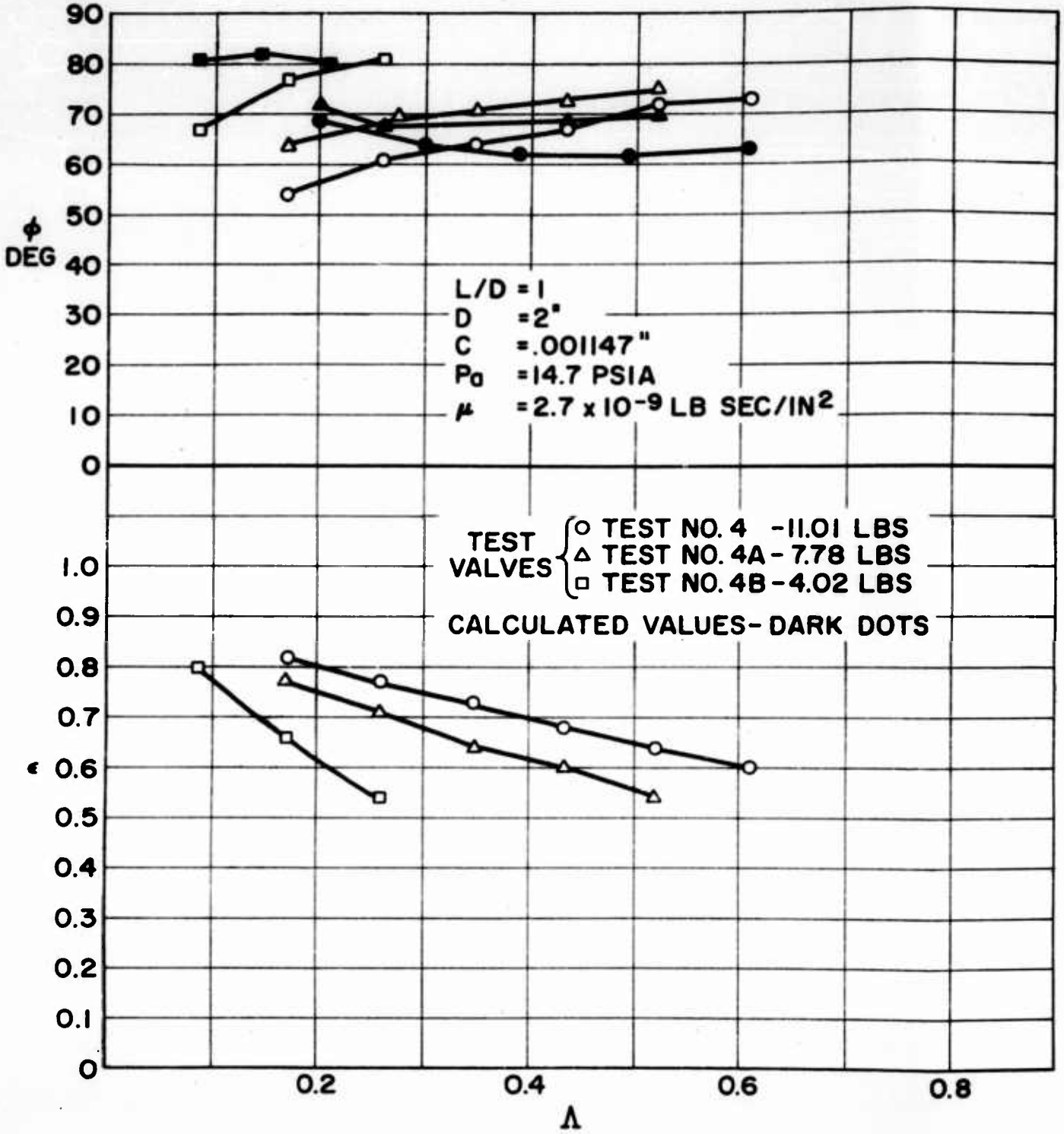

Fig. 9. Plots of Ø and ε vs. Λ.

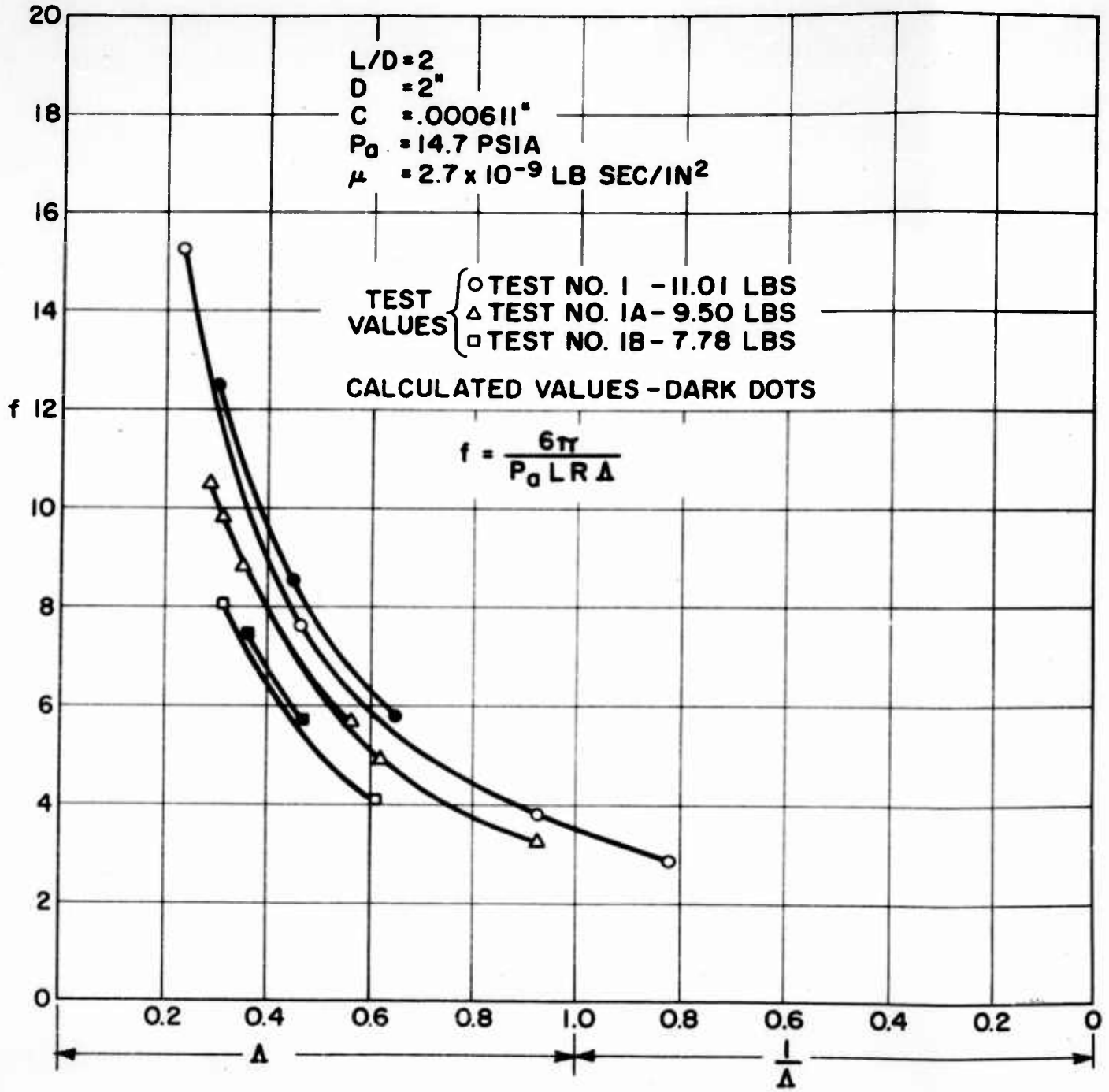

Fig. 10. Plots of Λ vs. f.

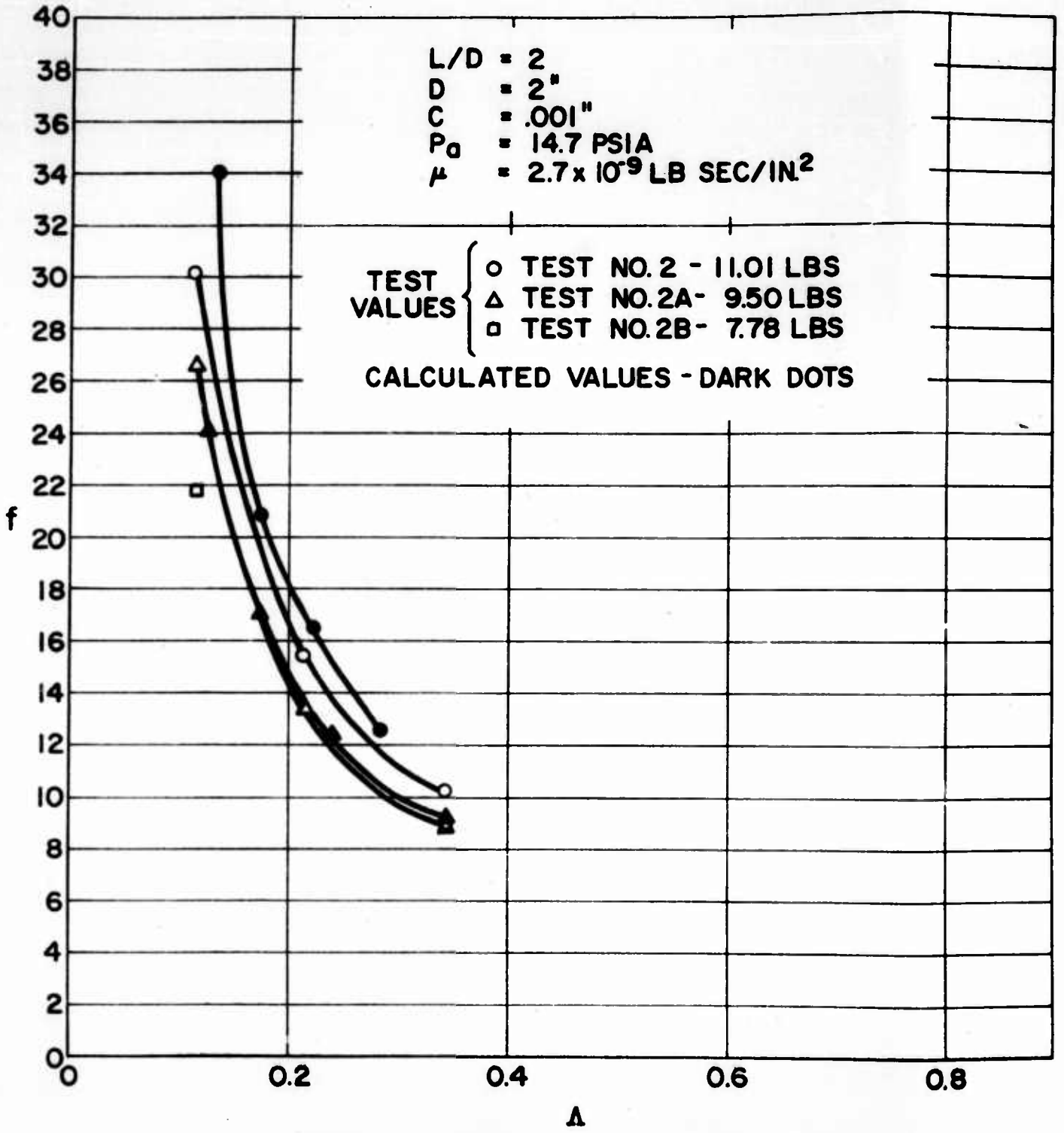

Fig. 11. Plots of Λ vs. f.

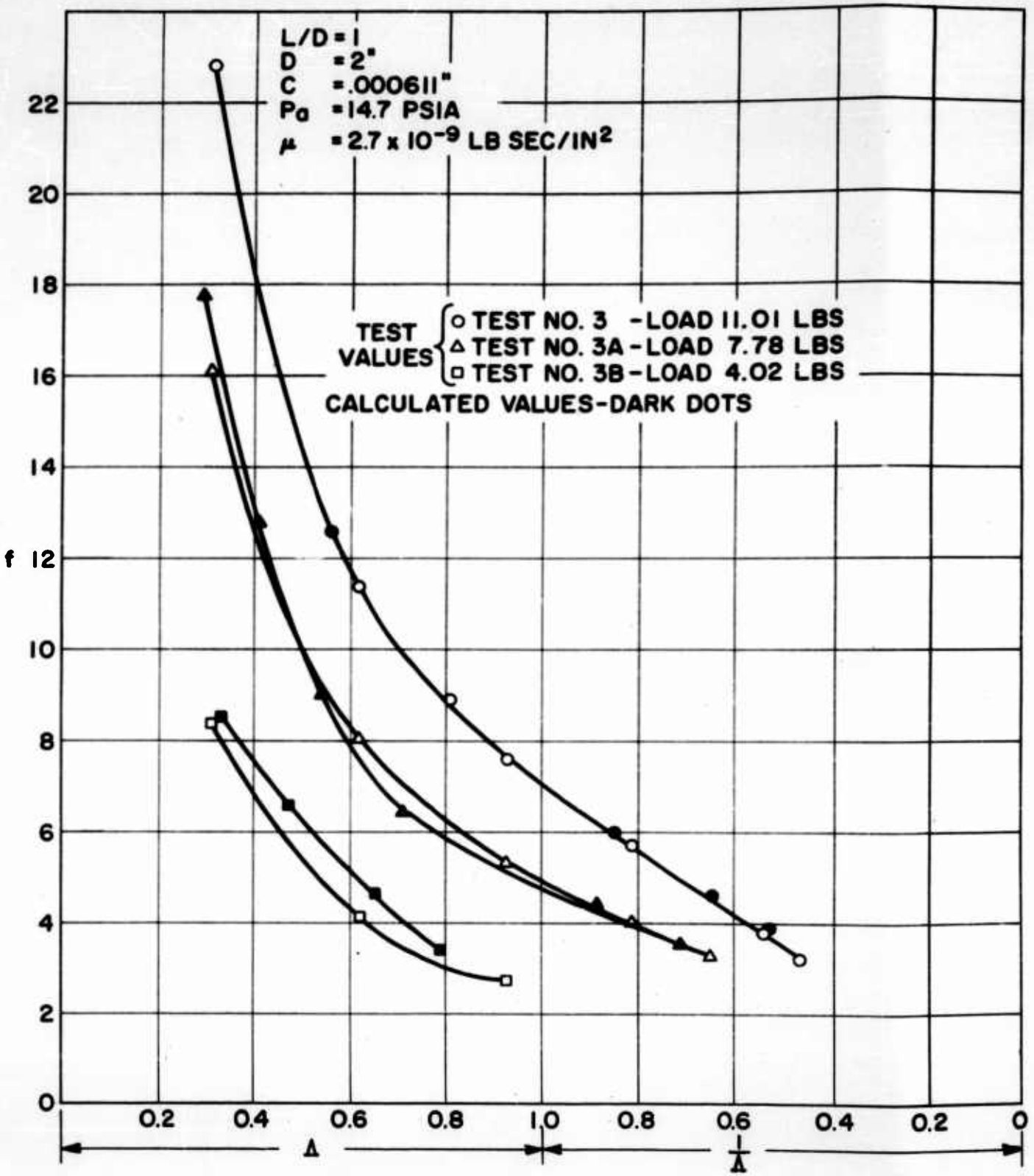

Fig. 12. Plots of Λ vs. f.

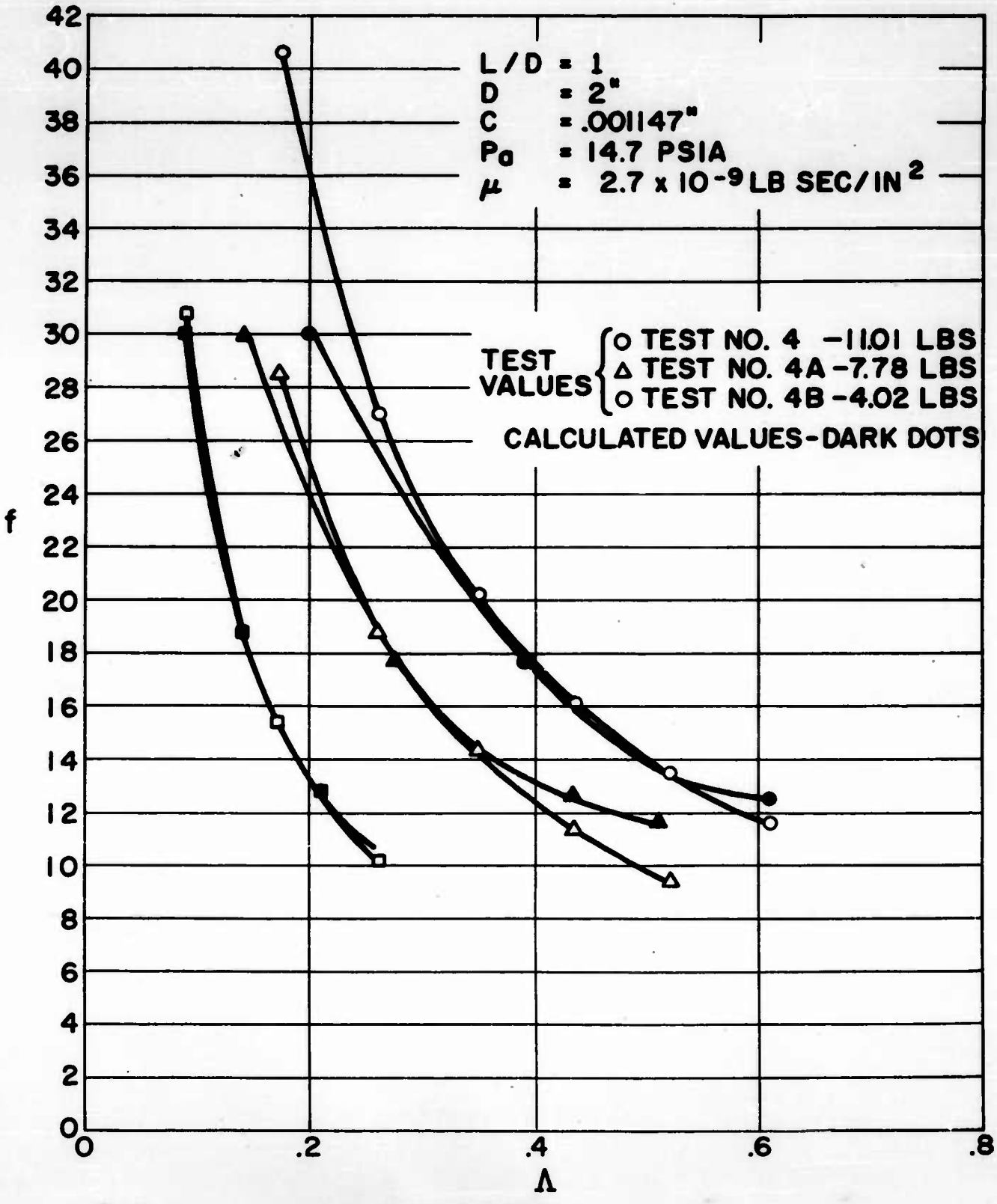

Fig. 13. Plots of Λ vs. f.

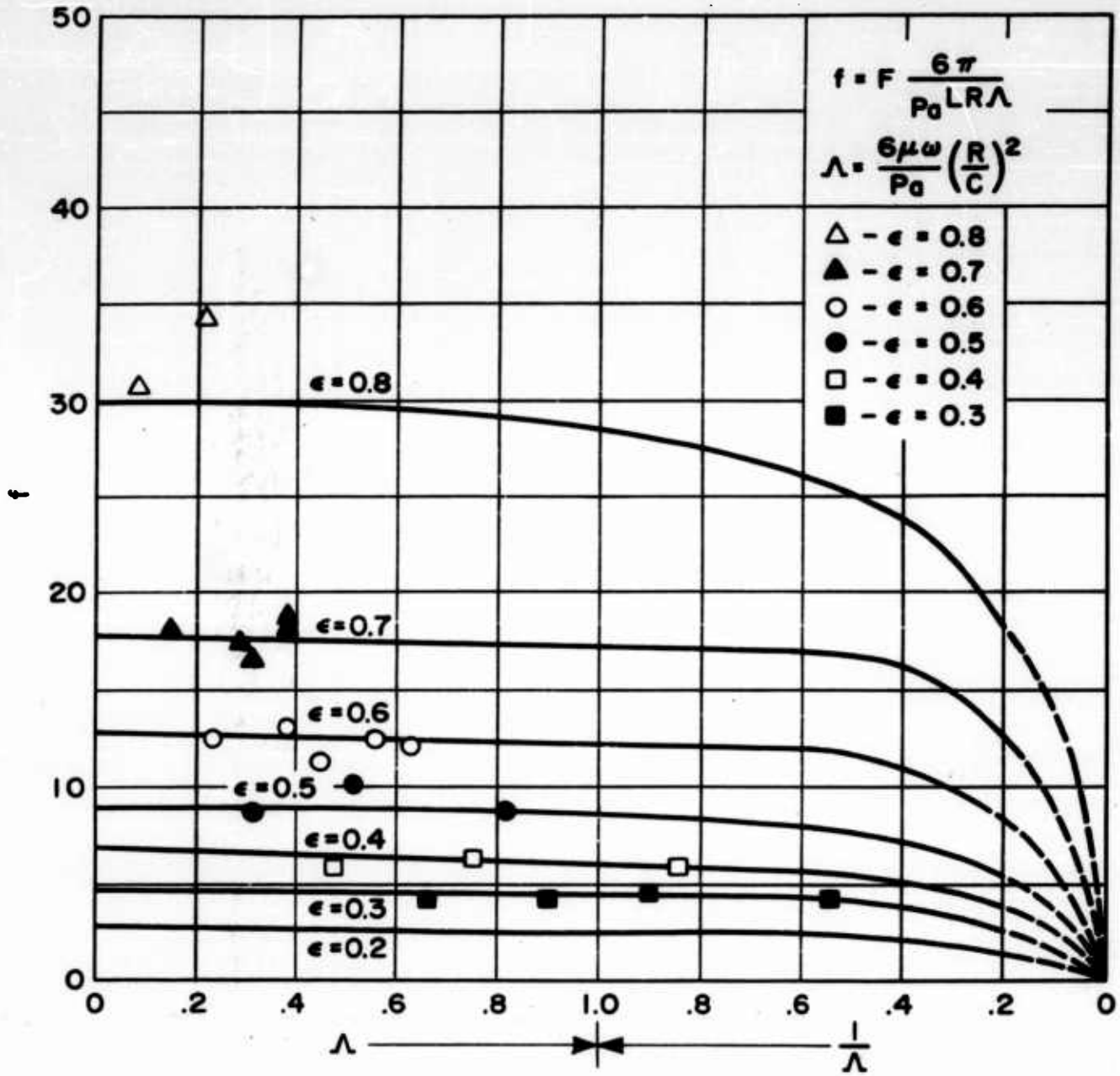

DIMENSIONLESS FORCE VS COMPRESSIBILITY NUMBER FOR L/D=1

Fig. 14. Plots of Λ vs. f at different eccentricity ratios for L/D = 1 and L/D = 2 respectively.

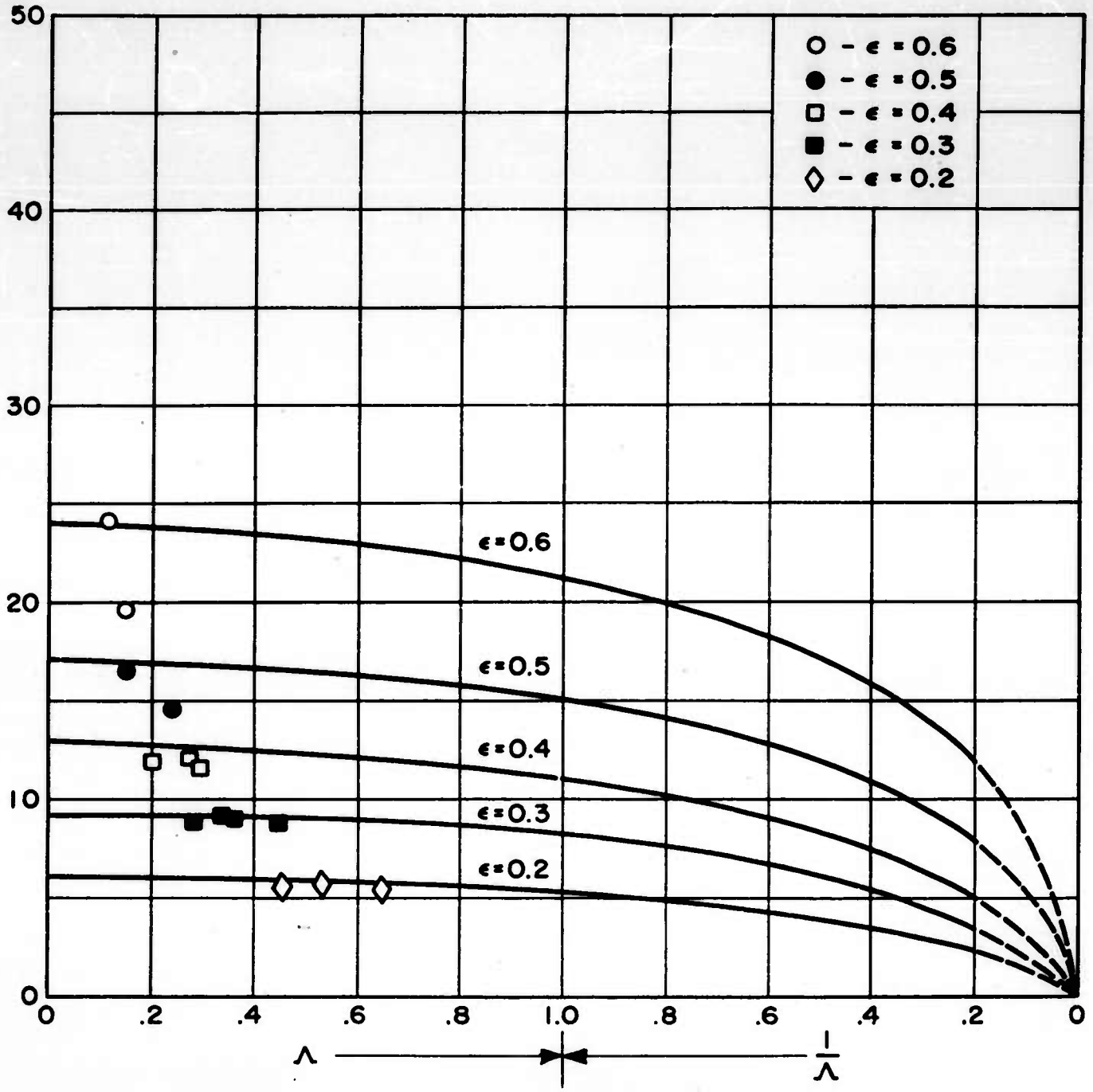

Fig. 15. Plots of Λ vs. f at different eccentricity ratios for L/D = 1 and L/D = 2 respectively.

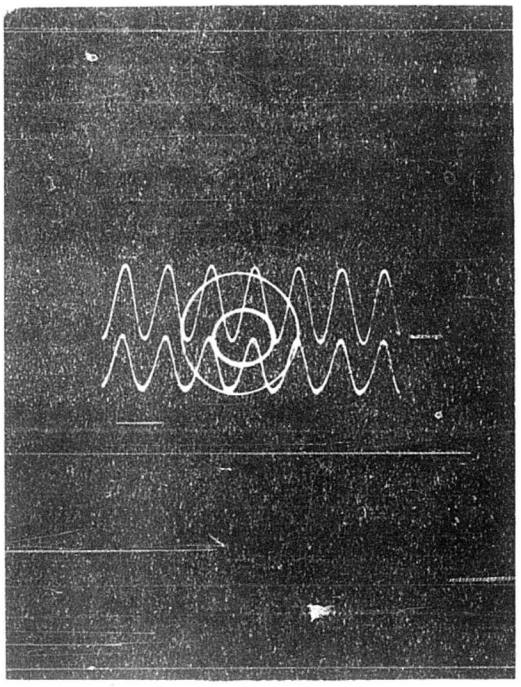

FIGURE 16

ONSET OF HALF FREQUENCY WHIRL 7700 RPM

PICTURE TAKEN AT 7800 RPM

Translatory Whirl

Turbine End Whirl Amplitude .0004"
Other End Amplitude .0008"

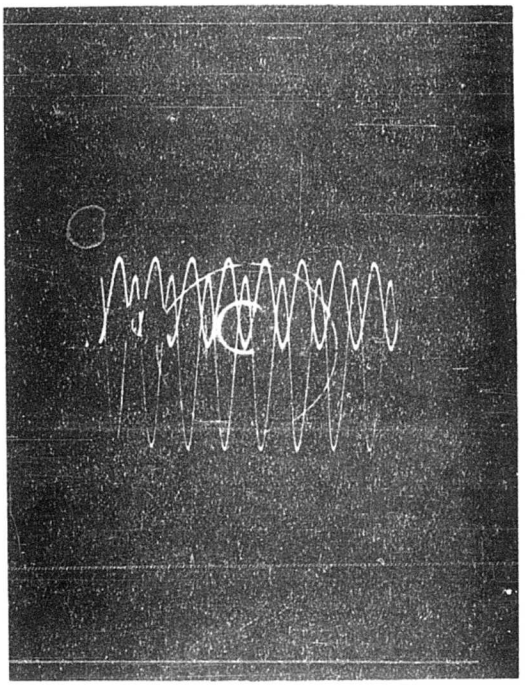

FIGURE 17

SAME RUN AS IN FIGURE 16

PICTURE TAKEN AT 9000 RPM

Conical Whirl

Turbine End Whirl Amplitude .00115"
Other End Amplitude .00035"

L = 4", D = 2", C = .000611"
Load = 11.01 #/bearing

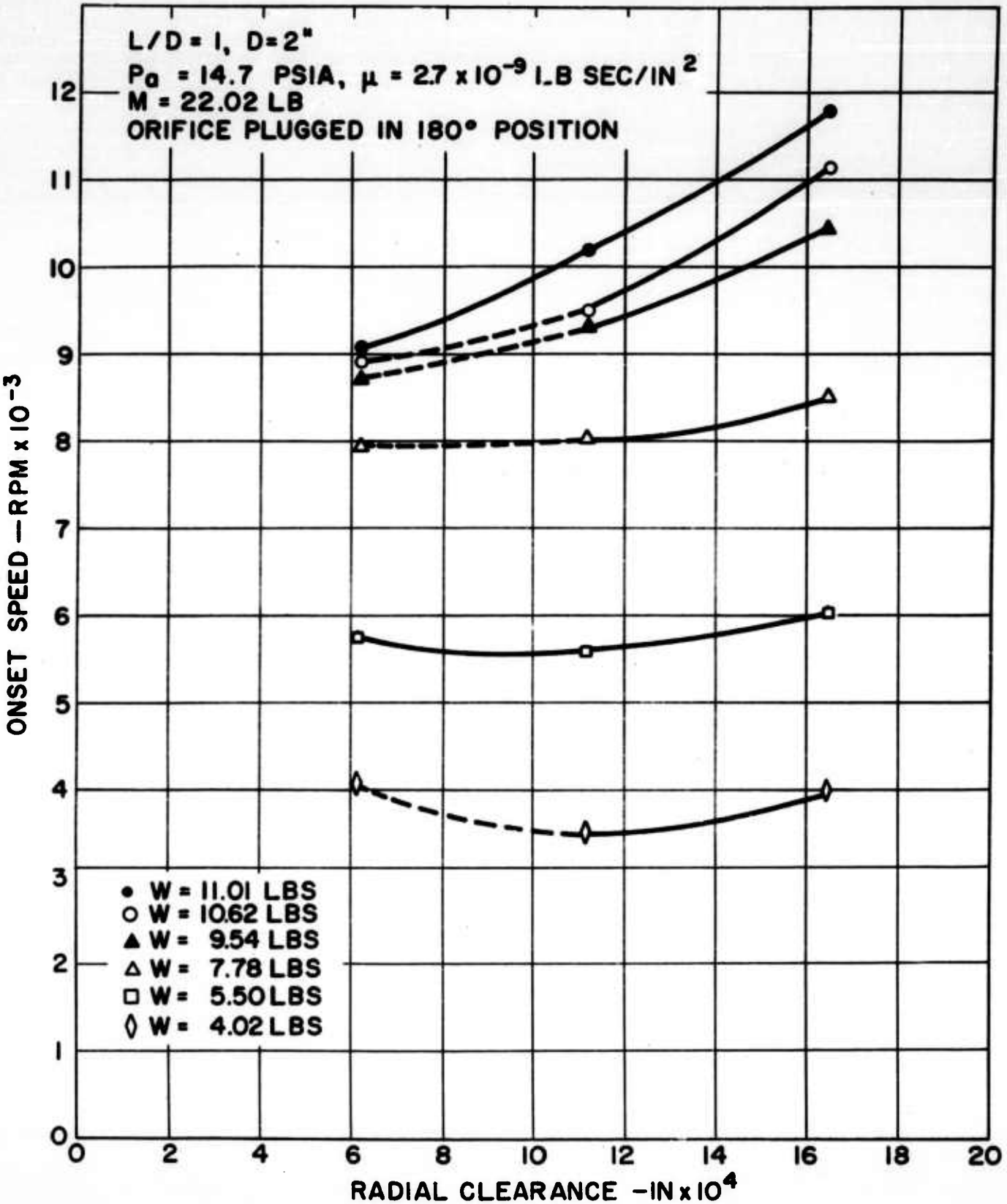

Fig. 18. Onset of HFW as function of load and clearance, L/D = 1.

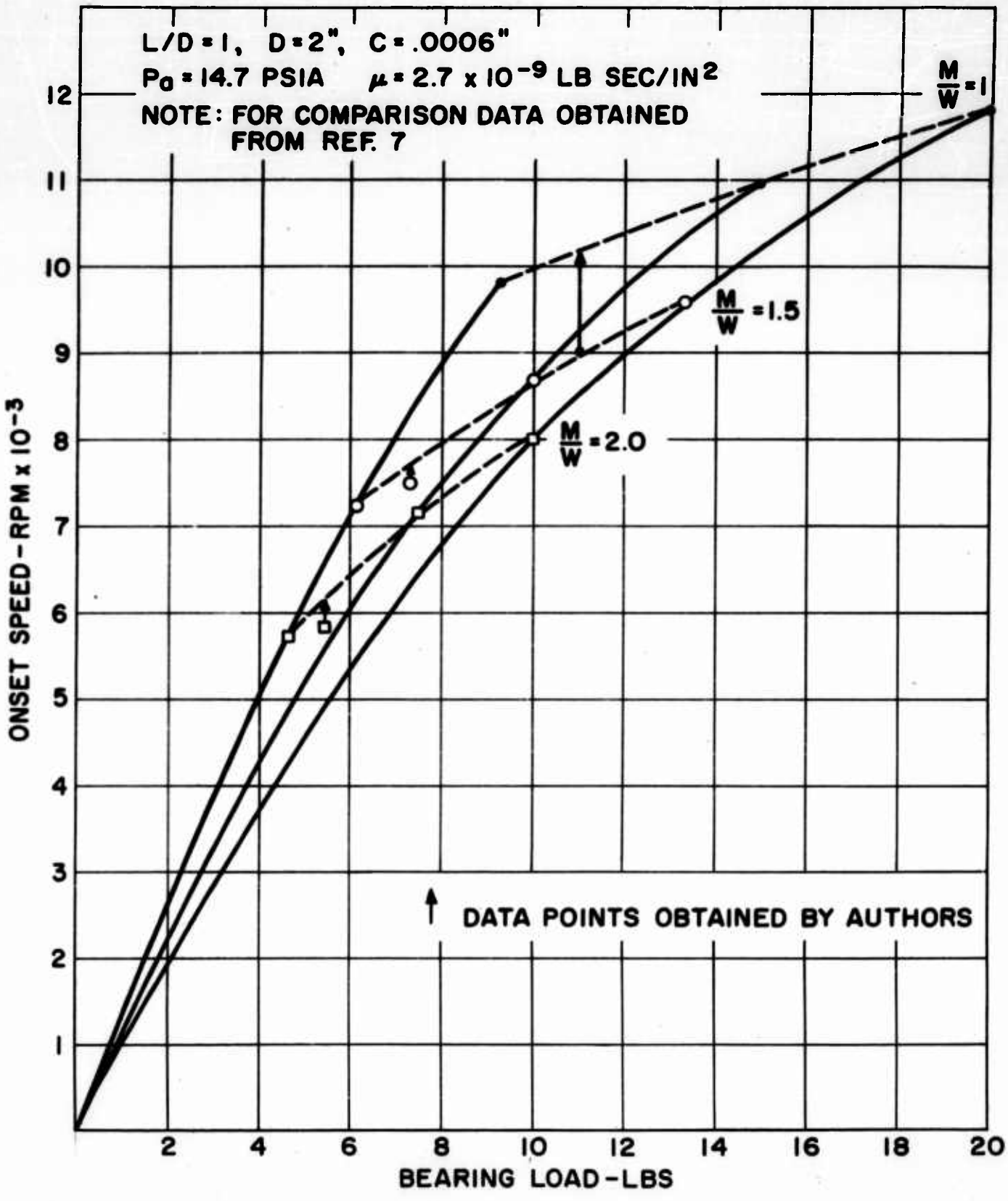

Fig. 19. Onset of HFW vs. bearing load for L/D = 1, C = 0.0008".

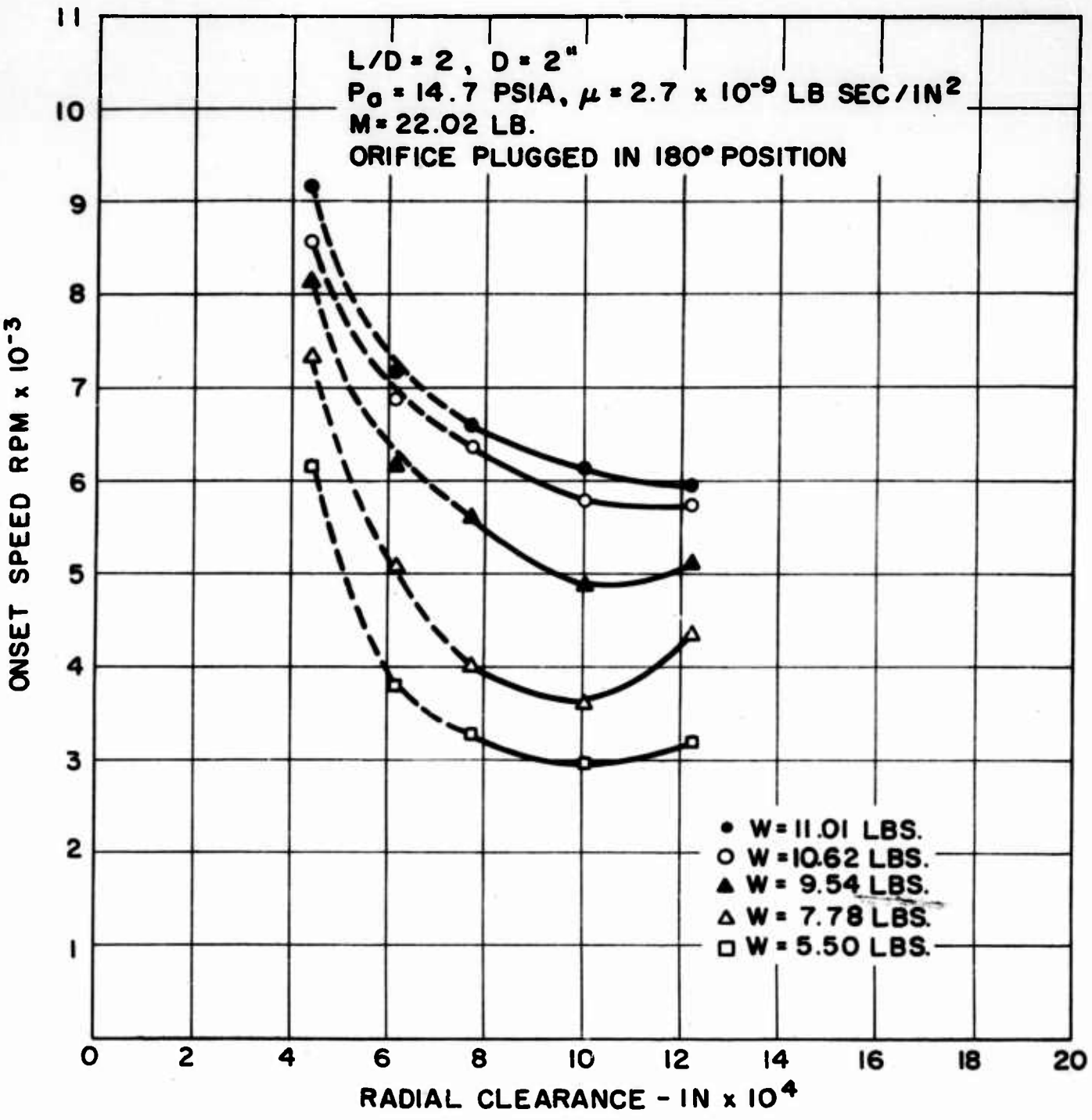

Fig. 20a.. Onset of HFW as function of clearance and load, L/D = 2.

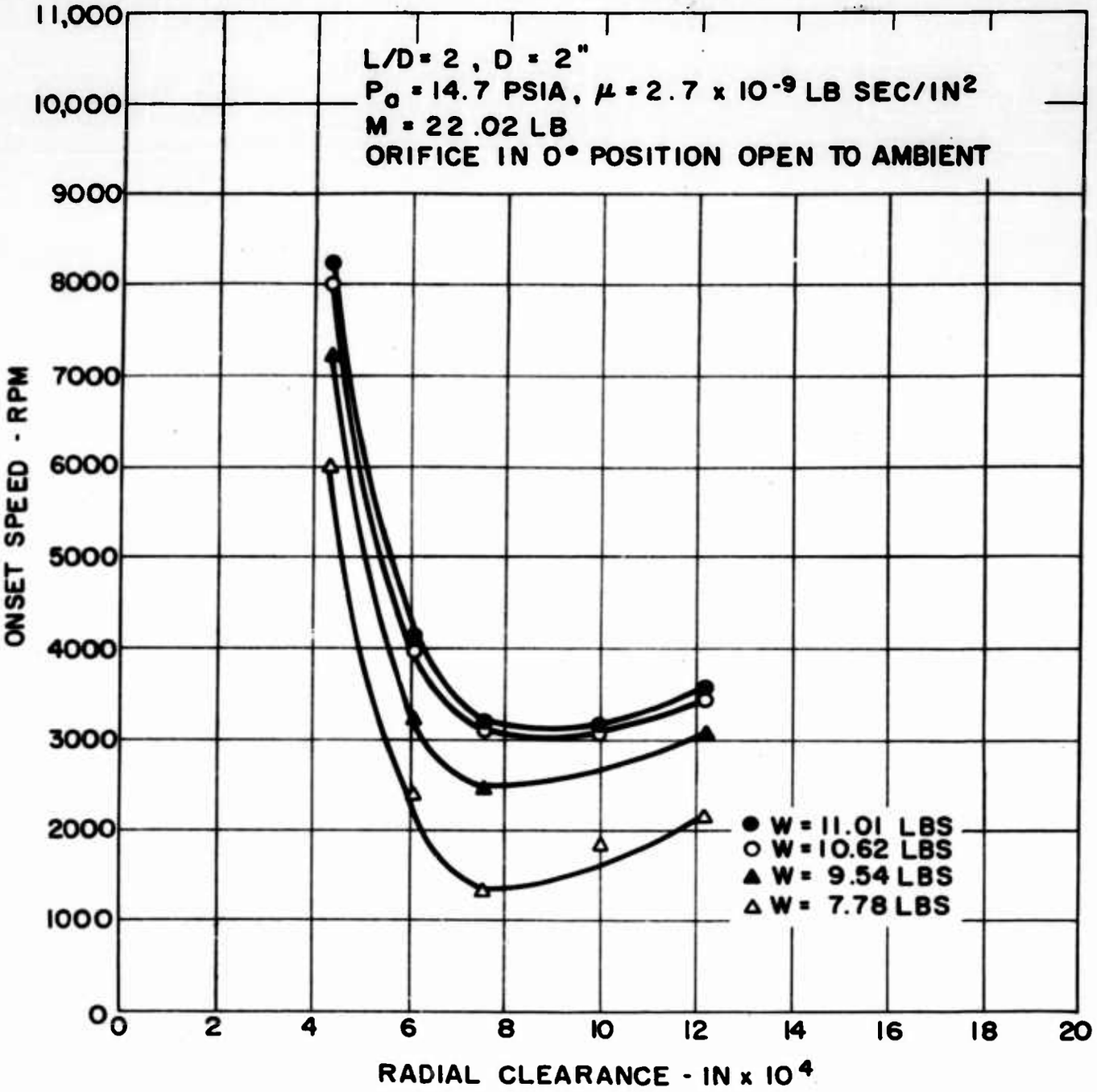

Fig. 20b. Onset of HFW as function of clearance and load, L/D = 2.

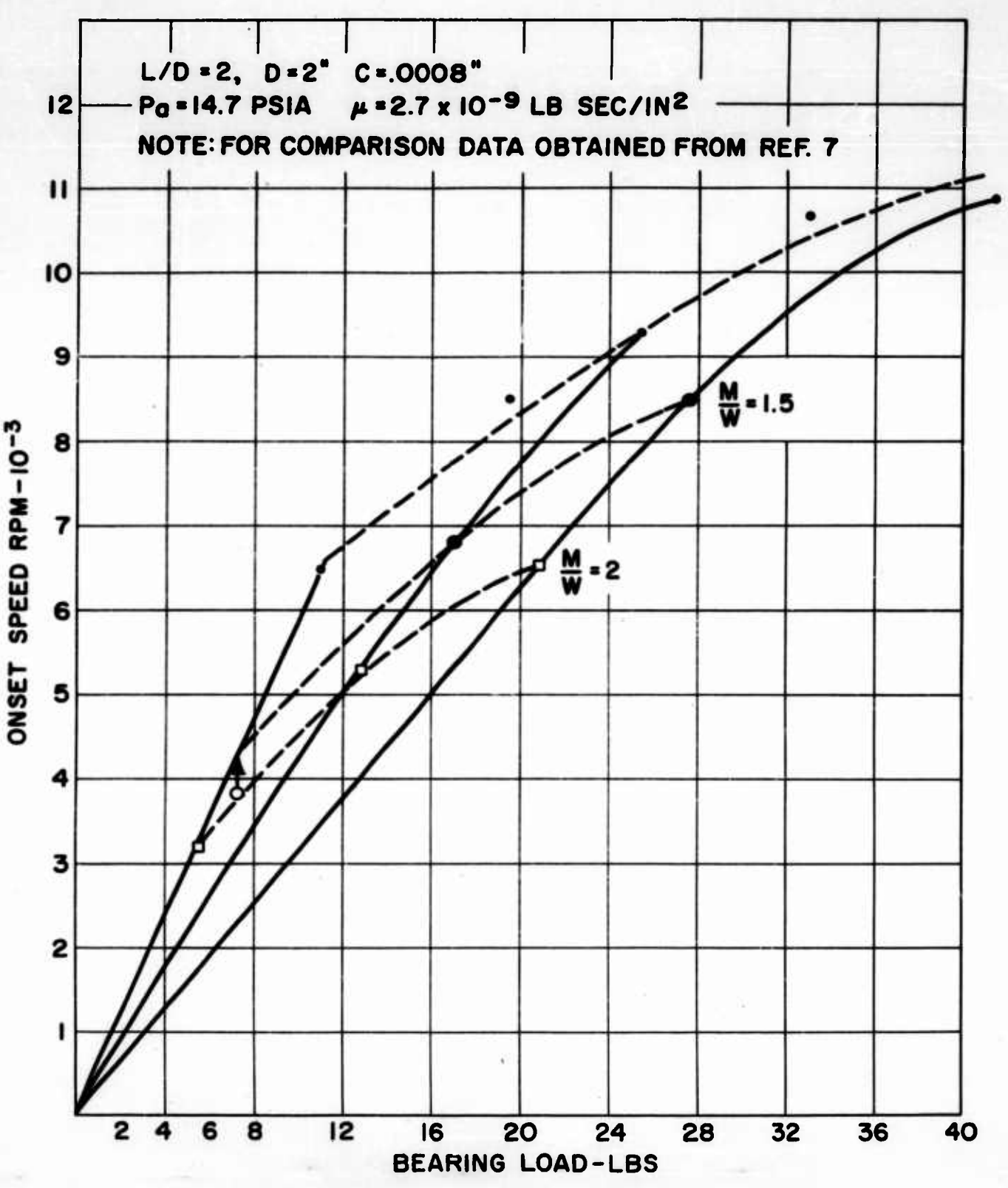

Fig. 21. Onset of HFW vs. bearing load for L/D = 2, C = 0.0008".

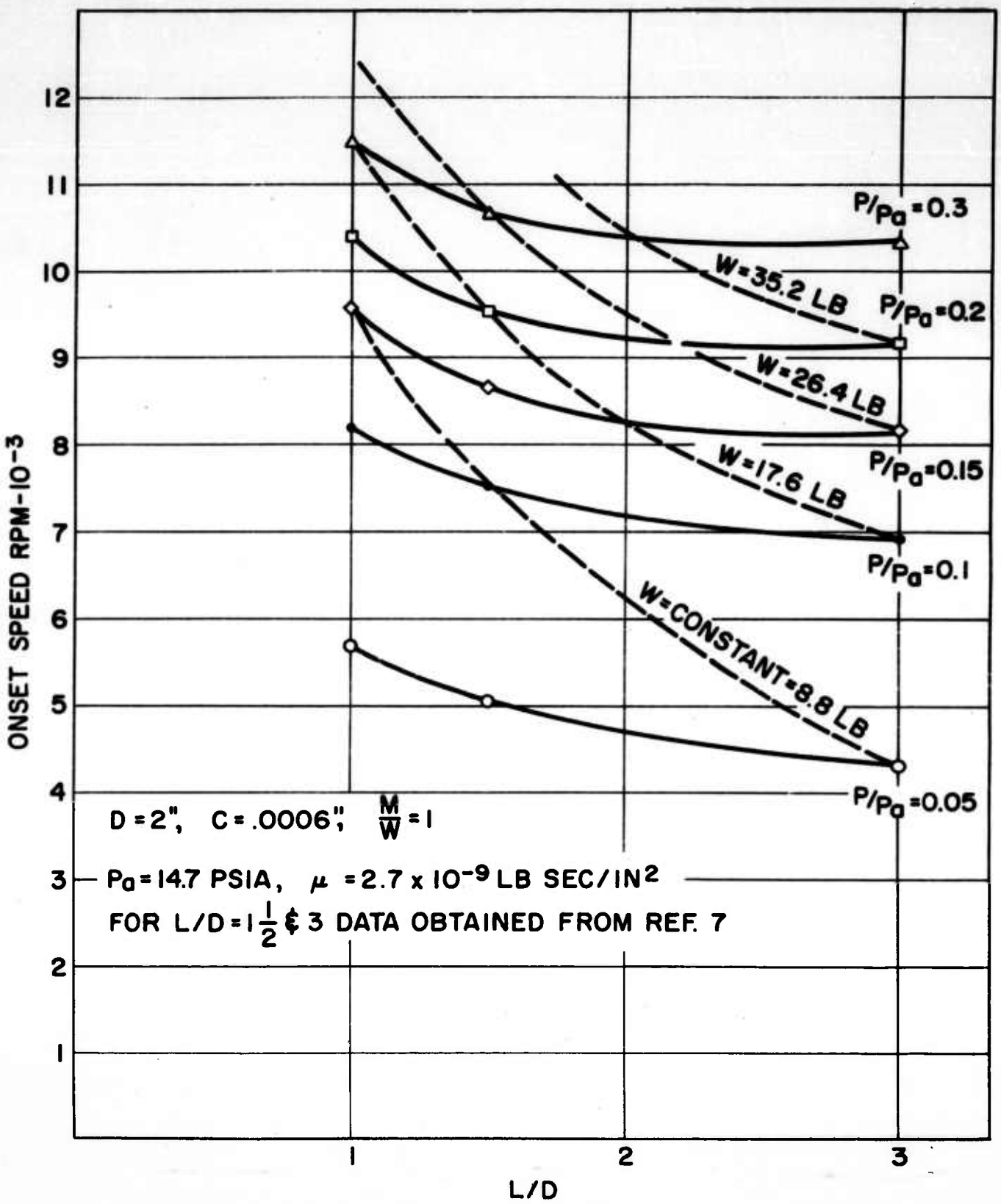

Fig. 22. Stability curves C* vs ω* for b = 1.

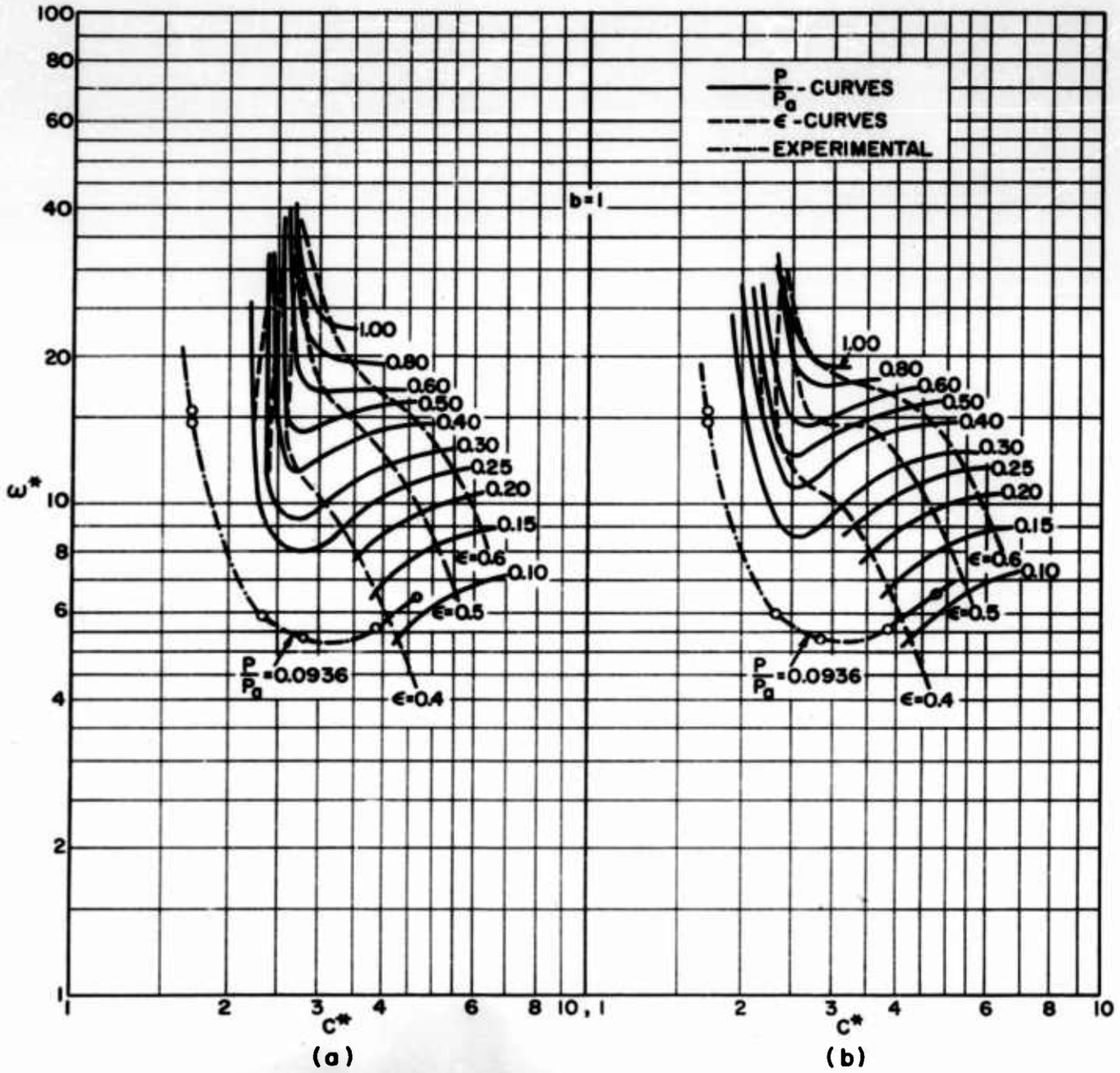

Fig. 23. Onset of HFW vs. L/D for C = .0006", M/W = 1.

APPROVED DISTRIBUTION LISTS FOR UNCLASSIFIED TECHNICAL REPORTS ISSUED UNDER GAS LUBRICATED BEARINGS CONTRACTS

Contract NONR 2844(00) NR 061-112

Chief of Naval Research
Department of the Navy
Washington 25, D. C.
Attn: Code 438 — 10
461 — 1
423 — 1
429 — 1
463 — 1
466 — 1

Commanding Officer
Office of Naval Research
Branch Office
346 Broadway
New York 13, New York — 1

Commanding Officer
Office of Naval Research
Branch Office
1030 East Green Street
Pasadena 1, California — 1

Commanding Officer
Office of Naval Research
Branch Office
Tenth Floor
The John Crerar Library Bldg.
86 East Randolph Street
Chicago, Illinois — 1

Commanding Officer
Office of Naval Research
Branch Office
Navy No. 100 Fleet Post Office
New York, New York — 10

Office of Naval Research
Resident Representative
University of Pennsylvania
Room 213, Hare Building
Philadelphia 4, Pennsylvania — 1

Director
Naval Training Device Center
Sands Point, Port Washington
Long Island, New York — 1

Chief, Bureau of Ships
Department of the Navy
Washington 25, D. C.
Attn: James C. Reid (Code 644B) — 8

Material Laboratory Library
Building 291, Code 912B
New York Naval Shipyard
Brooklyn 1, New York — 1

Director
Naval Research Laboratory
Washington 25, D. C.
Attn: Code 5230 — 1
2000 — 6

Director
U.S. Naval Engrg. Experiment Station
Annapolis, Maryland
Attn: Supervisor, Bearings Project,
Code 790 — 2

Commanding Officer
U.S. Naval Boiler and Turbine Lab.
Naval Base
Philadelphia, Pannsylvania — 1

Commanding Officer
U.S. Naval Avionics Facility
Indianapolis 18, Indiana
Attn: J.G. Weir — 1

Superintendent
U.S. Naval Postgraduate School
Monterey, California — 1

Commanding General
U.S. Army Engineer R and D Labs.
Fort Belvoir, Virginia
Attn: W.M. Crim, Nuclear Power
Field Office — 2
Technical Intelligence Br. — 1

Office of Chief of Ordnance
Research and Development Division
Department of the Army
Washington 25, D.C.
Attn: Normal L. Kleir

Chief, Bureau of Naval Weapons
Department of the Navy
Attn: G. D. Norman (RAAE-343) 3
L. Schlesinger (RREN-4) 3

Chief of Research and Development
Office, Chief of Staff
Department of the Army
Pentagon Building
Washington 25, D. C. 1

Commanding Officer
U.S. Army Research Office
(DURHAM)
Box CM, Duke Station
Durham, North Carolina 1

Commanding Officer
Detroit Arsenal
Centerline, Michigan
Attn: ORD MX-ECPD 1

Commander
Army Rocket and Guided Missile
Agency
Redstone Arsenal, Alabama
Attn: Technical Library,
ORDXR-OTL 1

Committee on Equipment and
Supplies
Office of the Assistant Secretary
of Defense (R and D)
The Pentagon
Washington 25, D. C. 1

Armed Services Technical
Information Agency
Arlington Hall Station
Arlington 12, Virginia
Attn: TIPCR 10

Commander
Aeronautical Systems Division
of the AirForce Systems Command
Wright Patterson AF Base, Ohio
Attn: WWRMFP-1, W. H. Biedenbender 1
WWRMPF-2, G. A. Beane 1
WWRMDD, P. C. Hanlon 1
ASRCEF-2, J. L. Morris 2

Headquarters
Wright Air Development Division
Air Research and Development Command
United States Air Force
Wright-Patterson AF Base, Ohio
Attn: WWRNGC-k, Phil Eignor 1

Commander
Air Force Office of Scientific
Research
Washington 25, D. C.
Attn: Joseph E. Long (SRDA) 3

Director
National Aeronautics and Space
Administration
1512 H Street, N. W.
Washington 25, D. C.
Attn: Harold Hessing 2

Chief of Staff, U.S. Air Force
The Pentagon
Washington 25, D. C.
Attn: DCS/D AFDRD/AD-2 1
DCS/D AFOP-OO 1

Commander
Air Research and Development Command
Andrews Air Force Base
Washington 25, D. C.
Attn: Lt. Col. C. D. Reifstech, RADTAP 1

Army Reactors Branch
Reactor Development Division
U.S. Atomic Energy Commission
Washington 25, D. C.
Attn: Mr. Clarence Miller 2

Technical Library
U.S. Atomic Energy Commission
Washington 25, D. C.
Attn: John L. Cook 3

Office of Maritime Reactors
Division of Reactor Development
Atomic Energy Commission
Washington 25, D. C.
Attn: Mr. S. Shiozawa 1

Chief, Division of Engineering
Maritime Administration
GAO Building
Washington 25, D. C. 1

General Engineering Laboratory
General Electric Company
One River Road
Schenectady 5, New York
Attn: Dr. G.M. Rentzepis 1

General Motors Corporation
Research Laboratories Division
Technical Center
Detroit 2, Michigan
Attn: Mr. Robert Davies
Asst. Supr of Bearings
Section 1

Grumman Aircraft Engineering Corp.
Bethpage, Long Island, New York
Attn: Mr. John Karanik, Chief
Systems Design Department 1

Illinois Institute of Technology
Chicago 16, Illinois
Attn: Prof. L.N. Tao 1

International Business Machine Corp.
Research Laboratory
San Jose, California
Attn: Dr. W.A. Gross 5

Franklin Institute
Laboratory for Research and Development
Philadelphia, Pennsylvania
Attn: Professor D.D. Fuller 5

International Telephone and
Telegraph Laboratories
15151 Bledsoe Street
San Fernando, California
Attn: Mr. G.B. Speen 1

Institute of Aeronautical Sciences
2 East 64th Street
New York, New York 1

Jack and Heintz, Inc.
207 East Laboratory, Public Roads Bldg.
Washington National Airport
Washington 1, D.C. 1

Kearfott Company
1378 Main Street
Clifton, New Jersey
Attn: Mr. Walter Carow 1

Koppers Company, Inc.
Metals Products Division
P.O. Box 626
Baltimore, Maryland
Attn: Mr. I.C. Kuchler 1

Lear, Incorporated
Grand Rapids Division
110 Ionia Avenue, N.W.
Grand Rapids 2, Michigan 1

Lear, Incorporated
3171 South Bundy Drive
Santa Monica, California
Attn: Richard M. Mock, President 1

Litton Industries
336 North Foothill Road
Beverly Hills, California
Attn: Mr. D. Moors, Dept. 21 1

Lockheed Aircraft Corporation
Missiles and Space Division
P.O. Box 504
Sunnyvale, California
Attn: Dr. M.A. Steinberg, 53-30
Building 202, Plant 2, PA 1

Lycoming Division
Avco Manufacturing Corp.
Main Street
Stratford, Connecticut
Attn: Mr. S.B. Withington
President and General Manager 1

McDonnell Aircraft Corporation
Lambert St. - St. Louis Municipal
Airport
Box 516
St. Louis 3, Missouri
Attn: Mr. Kendall Perkins
Vice President (Engr.) 1

Marquardt Aircraft Company
P.O. Box 2013-South Annex
Van Nuys, California
Attn: Mr. A.J. Kreiner, Director
Controls and Accessories Div. 1

Massachusetts Institute of Technology
Room 35-132
Cambridge 39, Massachusetts
Attn: Prof, Milton C. Shaw
Depart, of Mechanical Engrg. 1

Jet Propulsion Laboratory
California Institute of Technology
4800 Oak Grove Avenue
Pasadena, California
Attn: Engineering Library 1
Dr. John H. Laub

Chief, Technical Information
Service Extension
P.O. Box 62
Oak Ridge, Tennessee
Attn: Melvin S. Day 1/repro

Head, Experimental Engineering,
R.P.D.
Oak Ridge National Laboratory
Building 9201-3
Oak Ridge, Tennessee
Attn: H.W. Savage 1

Commanding Officer
Diamond Ordnance Fuze Laboratories
Washington 25, D.C.
Attn: Technical Reference Section
(ORDTL 06.33) 1

Office, Chief of Engineers
Engineer R and D Division
Gravelly Point
Washington 25, D.C. 1

SP 23-Guidance
U.S. Navy
Washington, D.C.
Attn. D. Gold 2

Office of Technical Services
Department of Commerce
Washington 25, D.C. 1

A.C. Spark Plug Division
General Motors Corporation
Milwaukee 1, Wisconsin
Attn: Allen Knudsen 1

A.C. Spark Plug Division
General Motors Corporation
Route 128
Wakefield, Massachusetts
Attn: W.H. St. Laurent 1

Aerojet-General Corporation
Nucleonics
San Ramon, California 1

AiResearch Manufacturing Division
The Garrett Corporation
9851 S. Sepulveda Boulevard
Los Angeles, California
Attn: Jerry Glaser, Supervisor
Mechanical Lab. Dept. 93-17 1

Allis Chalmers Manufacturing Co.
Buda Division
1126 South 70th Street
Milwaukee 1, Wisconsin
Attn: Mr. Will Mitchell, Jr.
Acting Director of Research
Research Division 1

American Society of Lubrication Engrgs.
5 North Wabash Avenue
Chicago 2, Illinois 1

Chairman, Research Committee on
Lubrication
American Society of Mechanical Engrs.
29 West 39th Street
New York 18, N. Y. 1

Analogue Controls, Inc.
200 Frank Road
Hicksville, L.I., New York
Attn: Mr. J.L. Cherubim
Chief Engineer 1

Applied Physics Laboratory
Johns Hopkins University
Silver Spring, Maryland
Attn: George L. Seielstad,
Supr, Tech. Reports Group 1

Autonetics
A Division of N. American Aviation
9150 East Imperial Highway
Downey, California 1

The Barden Corporation
Danbury, Connecticut
Attn: B.L. Mims, Vice President 1

Battelle Memorial Institute
505 King Avenue
Columbus 1, Ohio
Attn: Dr. Russell Dayton 1

Beemer Engineering Company
401 North Broad Street
Philadelphia 8, Pa. 1

Maico Electronics, Inc.
21 North Third Street
Minneapolis 1, Minnesota
Attn: Mr. G.E. Adams
Automatic Controls Dept. 1

Massachusetts Institute of Technology
Department of Aeronautical Engineering
Instrumentation Laboratory
Cambridge 39, Massachusetts 2

Dynamic Analysis and Control Lab.
Massachusetts Institute of Technology
Cambridge 39, Massachusetts
Attn: Dr. R.W. Mann 1

Aeronautical Engineering Labs.
University of Michigan
Ann Arbor, Michigan
Attn: Prof. R.B. Morrison 1

Minneapolis-Honeywell Regulator Co.
Gyro Section
2600 Ridgeway Road
Minneapolis, Minnesota
Attn: Mr. Jack W. Lower
Chief, Aeronautical Div. 1

Cryogenic Engineering Laboratory
National Bureau of Standards
Boulder, Colorado
Attn: Mr. B.W. Birmingham 1
Library 1

U.S. Department of Commerce
National Bureau of Standards
Boulder Laboratories
Boulder, Colorado 1

New Departure
Division of General Motors Corp.
Briston, Connecticut
Attn: R.N.S. Schiedt, Manager
Bearing Development and Contract 1

Norden Laboratories
Norden Div. of United Aircraft Corp.
White Plains, New York
Attn: Miss Elizabeth Zeil, Librarian 1

Department of Chemical Engineering
New York University
New York 53, New York
Attn: James J. Barker, Assoc. Prof.
of Nuclear Engineering

New Hampshire Ball Bearings, Inc.
Peterborough, New Hampshire
Attn: Mr. Henry F. Villaume, Engr. 1

Northrop Corporation
Norair Division
1001 East Broadway
Hawthorne, California
Attn: Library, 3145-31 1

Nortronics
A Division of Northrop Corporation
100 Morse Street
Norwood, Massachusetts
Attn: Mr. E. L. Swainson, Tech. Asst.
Precision Products Dept. 1

The Technological Institute
Northwestern University
Evanston, Illinois
Attn: Professor A. Charnes 1

Pratt and Whitney Aircraft Div. CANEL
P.O. Box 1102
Middletown, Connecticut 1

Radio Corporation of America
Camden, New Jersey 1

Ryan Aeronautical Company
Lindberg Field
San Diego 12, California
Attn: Mr. Frank W. Fink
Vice Pres. and Chief Engr. 1

Sanderson and Porter
72 Wall Street
New York 5, New York
Attn: Mr. S.T. Robinson

Solar Aircraft Company
2200 Pacific Highway
San Diego 12, California
Attn: Paul A. Pitt, Chief Engineer 1

Space Technology Laboratories, Inc.
P.O. Box 95001
Los Angeles 45, California
Attn: Mr. Kenton Andrews
Bldg. "F", Room 125 1

Sperry Gyroscope Company
Div. Of Sperry Rand Co.
Great Neck, L.I., New York
Attn: Mr. Wilmer L. Borrow
Vice President for R and D 1

Utica Division
Bendix Aviation Corporation
Utica, New York
Attn: Mr. Russell T. DeMuth,
Senior Engr. 1

Bendix Aviation Corporation
Research Laboratories Division
Southfield, Michigan
Attn: Mr. Ralph H. Larson 1

Boeing Airplane Company
Research Group
Box 3707
Seattle 25, Washington
Attn: Mr. D.J. Melchior
Mechanical Equipment 1

Bryant Chucking Grinder Company
60 Clinton Avenue
Springfield, Vermont
Attn: Mr. Roald Cann 1

Cadillac Gage Company
P.O. Box 3806
Detroit 5, Michigan
Attn: Mr. J. Taylor, Project Engr. 1

Carrier Corporation
Division of Research
Research Center
Syracuse, New York
Attn: Dr. Dewey J. Sandell 1

Chance Vought Corporation
P.O. Box 5907
Dallas, Texas
Attn: Mr. R.C. Blaylock
Vice President, (Engr) 1

Chrysler Corporation
Defense Operations
P.O. Box 757
Detroit 31, Michigan
Attn: Mr. C.W. Snider 1

The Cleveland Graphite Bronze Co.
17000 St. Clair Avenue
Cleveland 10, Ohio
Attn: Mr. R.H. Josephson 1

Collins Construction Co.
P.O. Box 86
Port Lavaca, Texas
Attn: Mr. James D. Mamarchev
Consulting Engineer 1

Convair
A Division of General Dynamics Corp.
Fort Worth, Texas
Attn: Mr. L.E. McTaggart, Sr.Des.Engr.
Engrg. Annex No. 1 1

Curtiss-Wright Corp.
Wright Aeronautical Division
Department 8311
Wood Ridge, New Jersey
Attn: Mr. W.J. Derner,
Chief Project Engr. 1

Daystrom Pacific
9320 Lincoln Boulevard
Los Angeles 45, California
Attn: Robert H. Smith
Special Project Engr. 1

Dynamic Controls Corporation
14 Runde Lane
Bloomfield, Connecticut
Attn: Mr. Thomas P. Farkas 1

E.I. DuPont de Nemours and Co., Inc.
Wilmington 98, Delaware
Attn: Dr. McNeilly
Mechanical Development Lab. 1

Electronics Systems Laboratory
Federal Telecommunications Labs.
Nutley, New Jersey
Attn: Mr. John Metzger 1

Ford Instrument Co.
31-10 Thomson Avenue
Long Island City 1, New York
Attn: Mr. Jarvis

Ford Motor Company
Dearborn, Michigan
Attn: Prof. Adolph Egli 1

General Atomics Division
General Dynamics Corp.
P.O. Box 608
San Diego 12, California
Attn: Mr. F.W. Simpson 1

General Engineering Laboratory
General Electric Company
One River Road
Schenectady 5, New York
Attn: Dr. Beno Sternlicht

Sperry Gyroscope Company
1 x 115
Great Neck, L.I., New York
Attn: Mr. John W. Steves 1

Stevens Institute of Technology
Hoboken, New Jersey
Attn: Prof. P.F. Martinuzzi 1

Stratos Division
Fairchild Airplane and Engine Co.
Bay Shore, L.I., New York
Attn: Mr. George Mackowski 1

Sundstrand Turbo
2480 West 70th Avenue
Denver 21, Colorado 1

Thompson Ramo Wooldridge Corporation
P.O. Box 90534 Airport Station
Los Angeles 45, California
Attn: Mr. Robert I. King F1829 1

AiResearch Mfg. Co. of Arizona
P.O. Box 5217
Phoenix, Arizona
Attn: Librarian 2

Waukesha Bearings Corporation
P.O. Box 346
Waukesha, Wisconsin
Attn: Mr. J.M. Gruber, Ch. Engr. 1

Tribo-Netics Laboratories
Vermilion, Ohio
Attn: Mr. E. Fred Macks 1

Universal Match Company
Avionics Dept. Technical Library
4407 Cook Avenue
St. Louis 13, Missouri 1

USI Technical Center
3901 N.E. 12th Avenue
Pompano Beach, Florida
Attn: Dr. W.C. Knopf 1

School of Mechanical Engineering
University of Pennsylvania
Philadelphia 4, Pennsylvania
Attn: Prof. P.R. Trumpler, Director 1

Westinghouse Electric Corporation
Research Laboratories
East Pittsburg, Pennsylvania
Attn: Mr. John Boyd

Westinghouse Electric Corporation
P.O. Box 868
Pittsburg 30, Pennsylvania
Attn: Mr. J.K. Hardnette
Vice Pres. and General Manager 1

Worthington Corporation
Harrison, New Jersey
Attn: Mr. H. Walter
Director of Research 1

Litton Industries
336 North Foothill Road
Beverly Hills, California
Attn: Dr. J.S. Ausman 2

UNCLASSIFIED